A LANDSAT REMOTE SENSING STUDY OF VEGETATION GROWING

ON MINERALIZED TERRAIN

Thesis submitted for the degree of Doctor of Philosophy in

the University of London and the Diploma of Membership of

the Imperial College of Science and Technology

by

UBIRATAN PORTO DOS SANTOS

Department of Geology,
Royal School of Mines,
Imperial College of Science and Technology,
London, SW7 2BP.

1983

ABSTRACT

A Landsat Remote Sensing Study of Vegetation Growing on Mineralised Terrain

Ubiratan Porto dos Santos, 1983

This remote sensing study has been undertaken to examine the feasibility of using Landsat MSS data to detect geobotanically anomalous vegetation. The site selected was Shipham, Somerset, England, because it shows biogeochemical and geobotanical anomalies induced by a Zn, Pb, and Cd soil geochemical anomaly due primarily to the underlying lead-zinc mineralisation and secondarily to past mining activities. The vegetation cover, consisting of grasses and herb species, has anomalous contents of these metals that are variable according to the plant species and season, being higher in the winter months. However, the signs of plant metal stress that characterise the geobotanical anomaly such as reduced vegetation density and chlorosis are more apparent during late winter and early spring. Three Landsat MSS images, May 1977, March 1980, and October 1980, were registered and processed using an I^2S Digital Image Processing System. Their interpretations have shown that the geobotanical anomaly could be clearly detected on the spring image where it was noted to have higher visible and lower infrared reflectance in relation to the background vegetation, whereas on the other two images it was hardly distinguished from the background vegetation. The presence

of more apparent signs of plant metal stress during a particular phenological stage (spring leaf flush) seems to be the factor which increased differences in chlorophyll state and vegetation density and, hence, differences in spectral reflectance between the geobotanical anomaly and the background vegetation to a level that allowed its detection on the spring image. Though the spring image was the most useful to detect the Shipham geobotanical anomaly, its best visual discrimination was achieved by a multi-image enhancement technique (addition of multitemporal images), which may prove to be a valuable tool for interpreting similar seasonally pronounced geobotanical anomalies. An unsupervised computer-aided classification carried out using as input the multi-image enhancement was only partially successful. It is suggested that the utilisation of images acquired at several times of the year, with emphasis on the periods of phenological changes, coupled with a proper understanding of the seasonal pattern of plant metal stress of the area seems to offer the best possibilities for both detection and interpretation of geobotanical anomalies as a tool for mineral exploration.

ACKNOWLEDGEMENTS

CONTENTS

LIST OF FIGURES

LIST OF TABLES

CHAPTER ONE

INTRODUCTION

The idea of using vegetation as a guide to sub-surface geology and mineralisation has been investigated for centuries. The ancient prospectors were well aware of metal uptake and its physiological effects on plants for they observed the presence or absence of particular species or varieties of plants in mineralised areas and the effects of metals on plant growth, and used it in the search for hidden mineral deposits since the 8th century (Cannon, 1979). Nowadays, there are two different methodologies which use vegetation for prospecting. One is the visual observation of changes in plant morphology and distribution of species in order to define mineral prospects which is the oldest method and known as geobotany, whereas the other is biogeo-chemistry which was developed during the 1930's and uses chemical analysis of plant material to obtain evidence of mineralisation on the substrate.

Although the use of vegetation can be advantageous for prospecting in poorly exposed areas and specially useful in areas of transported overburden which would furnish little or no clue to mineralisation with conventional soil survey, its application has been hindered by the high degree of botanical skills required, the variety of environmental conditions influencing the growth of plants, and the need for time consuming orientation surveys and its local applic-ability.

However, the advent of remote sensing techniques have reduced the time and costs of surveying large areas for vegetation anomalies related to mineralisation, and hence brought a renewed interest in the geobotanical method of prospecting. Remote sensing can be broadly defined as the collection of information about an area through measurements of the electromagnetic energy emanating from it and made at some distance from it, usually at aircraft and satellite altitudes. The possibility of applying remote sensing techniques to geobotanical prospecting on a wide, even global, scale has obvious advantages for mineral exploration programmes. Moreover, the ability of modern remote sensing systems to collect ground information using regions of the electromagnetic spectrum beyond the visible (Fig. 1.1) in a multispectral fashion and, in the case of the Landsat satellite, the synoptic view over large areas and the repetitive sensing which allows the monitoring of vegetation on a seasonal basis, have provided a wealth of data that has further stimulated the increasing application of remote sensing to geobotanical studies.

This thesis aims at examining the feasibility of using Landsat MSS remote sensing data to detect geobotanically anomalous vegetation and to determine its spectral response pattern in relation to the surrounding vegetation. The site selected for study was Shipham, Somerset, England. This site was chosen because its vegetation canopy, consisting of grasses and herb species, shows biogeochemical and geobotanical anomalies that have been induced by high concentrations of Zn, Pb and Cd in the soil due primarily to
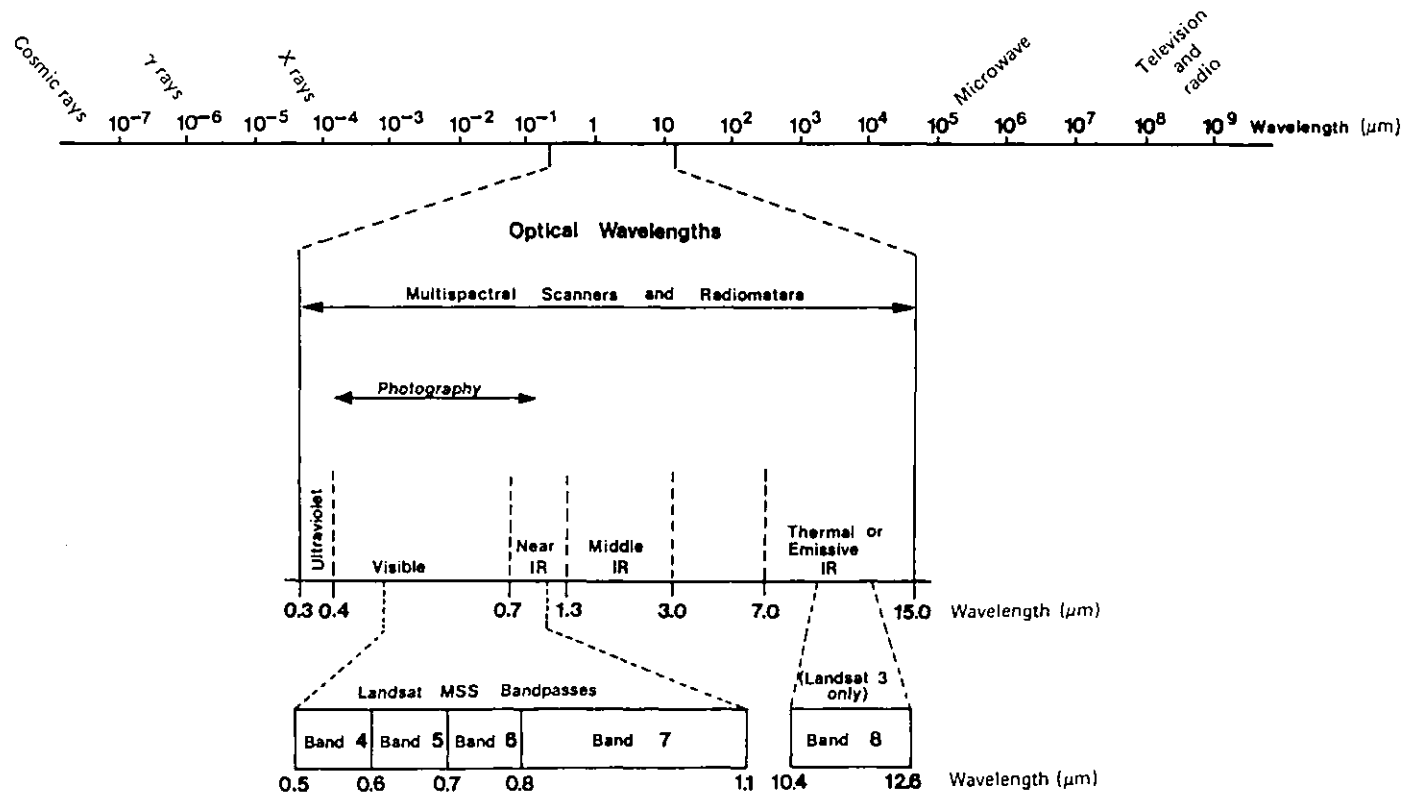
Figure 1.1 The eletromagnetic spectrum, showing in detail the region which can be sensed using optical instruments and the Landsat MSS bandpasses.

the underlying lead-zinc mineralization and secondarily to past mining activities that have ceased in the middle 19th century.

Three Landsat MSS images taken at different times of the year (late winter, spring, and autumn) were spatially registered and processed using an I^{2}S System 500 Digital Image Processing System. The image processing has been concerned with finding the best suited enhancement technique to increase image quality and make the geobotanically anomalous area more apparent on the imagery for detection and identification by visual interpretation. Additionally, an unsupervised computer-aided classification was performed to assess the degree of classification accuracy obtainable.

The other chapters of this thesis have the following contents: a detailed description of the characteristics of Landsat imagery (Chapter 2); an outline of the image processing techniques of remote sensing data and the approach followed in their utilisation (Chapter 3); a review of the biogeochemical and geobotanical methods of prospecting and of the application of remote sensing techniques to study geobotanical anomalies (Chapter 4); the results of the remote sensing study of the Shipham test site including a description of it, and the discussion of these results (Chapter 5); and the conclusions (Chapter 6).

CHAPTER TWO

LANDSAT IMAGERY

2.1   LANDSAT PROGRAMME

The Landsat Programme, first known as the Earth Resources Technology Satellite (ERTS) Programme, was conceived by a group of scientists in the U.S. Department of Interior and the National Aeronautics and Space Administration (NASA) during the 1960s. The aim of the programme was to launch a series of unmanned satellites to test the feasibility of acquiring multispectral remote sensing data on a systematic and repetitive manner in order to evaluate and monitor the earth's resources.

The first satellite, called ERTS-1, was launched on July 23, 1972, and it operated until January 6, 1978, far exceeding its one-year design life. The satellite carried a multispectral scanner (MSS), a return beam vidicon camera (RBV), two wide-band video tape recorders (WBVTR), and a data collection system (DCS). Because soon after launch one of the tape recorders and the RBV sensor developed malfunctions, preventing the use of this sensor, it was decided to launch a second satellite with the same sensor package as ERTS-1. The second satellite was launched on January 22, 1975. Concurrently the name of the satellite and programme was changed to emphasise its prime interest in the survey of the resources of the earth's land and to distinguish it from the planned Seasat oceanographic satellite programme. The second satellite was then called

Landsat 2, and the first was renamed Landsat 1. Landsat 2 operated until February 25, 1982. Landsat 3 was launched on March 5, 1978, and it carried sensor systems somewhat different than in the first two satellites.

The successful launch and operation of the Landsat satellites has provided the earth scientists with a valuable and prolific source of remote sensing data and has been an outstanding development in the field of remote sensing. Because of its global coverage, ready availability to any user, low price, and generally good quality, Landsat imagery has been increasingly applied worldwide to many practical earth's resources studies (NASA, 1973; NASA, 1974; Williams and Carter, 1976; Short, Lowman, Freden and Finch, 1976). The applications of Landsat data are found in such activities as oil and mineral exploration, land use monitoring and planning, forestry and rangeland management, agriculture, water management, environmental monitoring and pollution control, and cartography. Today 11 nations worldwide have the capability to directly receive and process data from Landsat and, in addition, more than 100 nations now make serious use of Landsat data for natural resources evaluation and management (NASA, 1982).

2.2   LANDSAT ORBIT CHARACTERISTICS

Landsat satellites are launched into a circular, near polar orbit with an inclination of 9 degrees, and at an altitude of approximately 920 km. They complete one orbit every 103 minutes, resulting in 14 orbits per day (Fig. 2.1). The distance between successive orbits is 2,760 km at
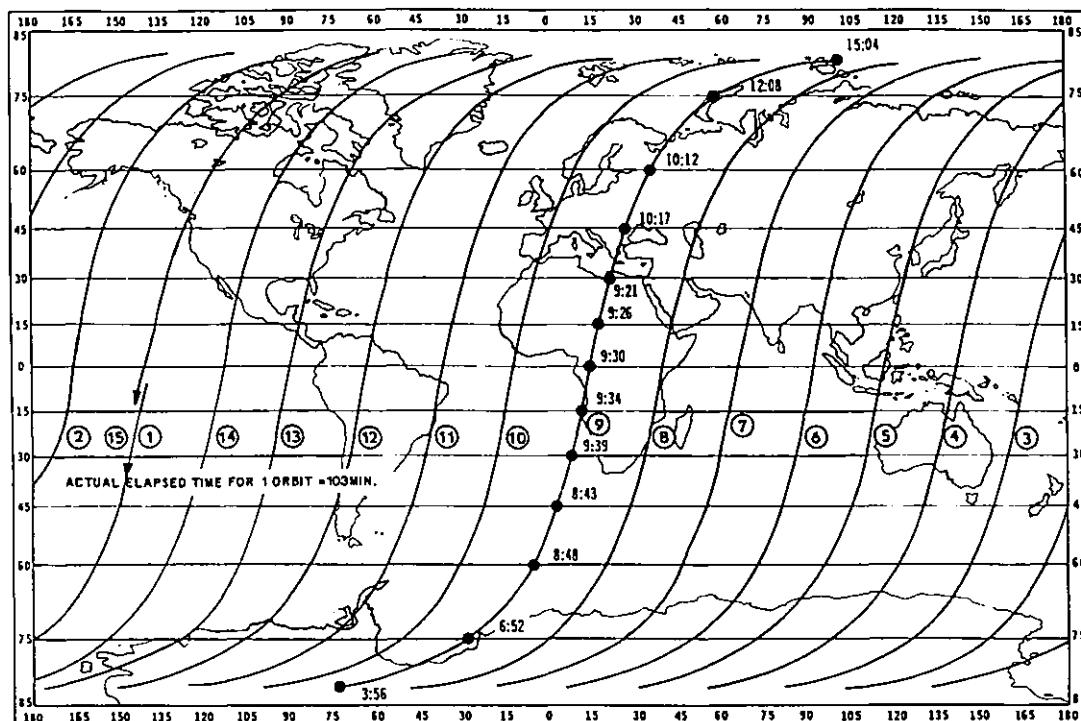
Figure 2.1 Typical Landsat daily orbit pattern, showing local time variation within an orbit. (From USGS, 1979).

the equator. Since the sensors aboard the satellite cover only a 185 km swath, there are large gaps in image coverage between successive orbits on a given day. However, with each new day the satellite orbit drifts westward, taking 18 days to reappear over the same spot. Thus, the satellite has the capability of covering the entire earth once every 18 days, or about 20 times per year. The coverage provided by Landsat sensors produce image sidelap between adjacent tracks, amounting to about 14 per cent at the equator and increasing with the increase in latitude, reaching 85 per cent at 80 degrees latitude.

The orbit of the Landsat satellites is sun synchronous to ensure repeatable solar illumination conditions, with a nominal 9.30 a.m. crossing of the equator on their descending path. Repeatable solar illumination

conditions are necessary for mosaicking adjacent tracks of imagery and for comparison of annual changes in land cover. Although Landsat has a sun synchronous orbit which ensures repeatable solar illumination conditions, these conditions vary with location and season because sun elevation angle and azimuth change as a function of latitude and time of the year (Taranik, 1977).

Landsat orbits are adjusted occasionally to compensate for orbital precession caused mainly by atmospheric drag and the gravitational attraction of the sun and moon. These adjustments, which are necessary to maintain the desired coverage pattern and repeatability characteristics of the system, are accomplished with a gas reaction system ensuring that repetitive image centres are maintained to within about 37 km of the nominal centres.

2.3   LANDSAT SENSORS

2.3.1   Introduction

The Landsat satellites carry two sensors on board: a return beam vidicon (RBV) camera system and a multi-spectral scanner (MSS). Two wide-band video tape recorders (WBVTR) are used to store the outputs of those systems when the satellites are out of range of a ground receiving station. The satellites also carry the relay antenna of the data collection system (DCS), which is used to relay environmental data such as temperature, stream flow, snow depth, soil moisture or volcano activity, from data collection platforms to ground stations.

2.3.2   Return Beam Vidicon (RBV) Camera System

The RBV system on board Landsats 1, 2 and 3 have all been similar in that they have utilised vidicon tube cameras, which use an electron beam to scan and read images stored on the photoconductive surface of the camera tube previously exposed by a shutter device, thus producing a video signal just as in a common television camera that can be recorded or telemetered to a ground receiving station.

On Landsats 1 and 2 the RBV system consisted of three vidicon cameras viewing simultaneously the same 185 km by 185 km ground area with a nominal ground resolution of 80 m and in three distinct spectral bands: 0.475 to 0.575 µm (blue-green-yellow); 0.580 to 0.680 µm (orange-red); and 0.690 to 0.830 µm (red-near infrared). Because of the early shutdown of the RBV system on Landsat 1 due to an electronic problem and its occasional operation on Landsat 2, this sensor saw little use, and consequently, the MSS became the prime sensor on board Landsats 1 and 2.

On Landsat 3, however, the RBV system consists of just two aligned vidicon cameras sensing adjacent areas of approximately 98 km by 98 km each, with a sidelap of 13 km. The nominal ground resolution is 24 m and both cameras sense the ground in a single broad band: 0.505 to 0.750 µm (green to near infrared). To achieve the same ground coverage as the MSS sensor, the two vidicon cameras are shuttered twice, sequentially, in the same time it takes for one MSS scene to be acquired, resulting in two pairs of subscenes, with an overlap of 16 km, for every MSS scene acquired. The RBV

system on Landsat 3 has been working normally and acquiring images with improved resolution compared to the MSS sensor, which should provide better discrimination of ground features. Unfortunately, the various sensor caused defects observed in many images (EROS Data Center, 1981) have prevented the availability of good quality RBV imagery and hence its use in the present work as planned.

2.3.3   Multispectral Scanner (MSS) System

2.3.3.1 MSS Characteristics and Operation

The MSS on board the Landsat satellites uses an oscillating mirror to scan the earth from west to east. The total field of view scanned is 11.56°, covering about 185 km on the ground (Fig. 2.2). The incoming radiation is reflected by the mirror into a telescope which focuses the radiation on an array of optical fibres. The fibres transfer the radiation to filters which allow only certain wavelengths to strike the detectors. The detectors then produce a voltage (an analog signal) proportional to the amount of radiation which is sampled every 9.95 microseconds and converted by a multiplexer to a digital number ranging from zero to 63 (6 bit byte).

The MSS spectral response is shown in Table 2.1. Each MSS spectral band utilises six detectors, so 24 detectors are used in the MSS. Photomultipliers are used as detectors for band 4, 5 and 6 and silicon photodiodes are used for band 7. The additional band, designated band 8, on

the Landsat 3 MSS uses just two Hg Cd Te detectors which are responsive to thermal infrared radiation. This thermal band failed soon after launch and for this reason will not be further mentioned here.
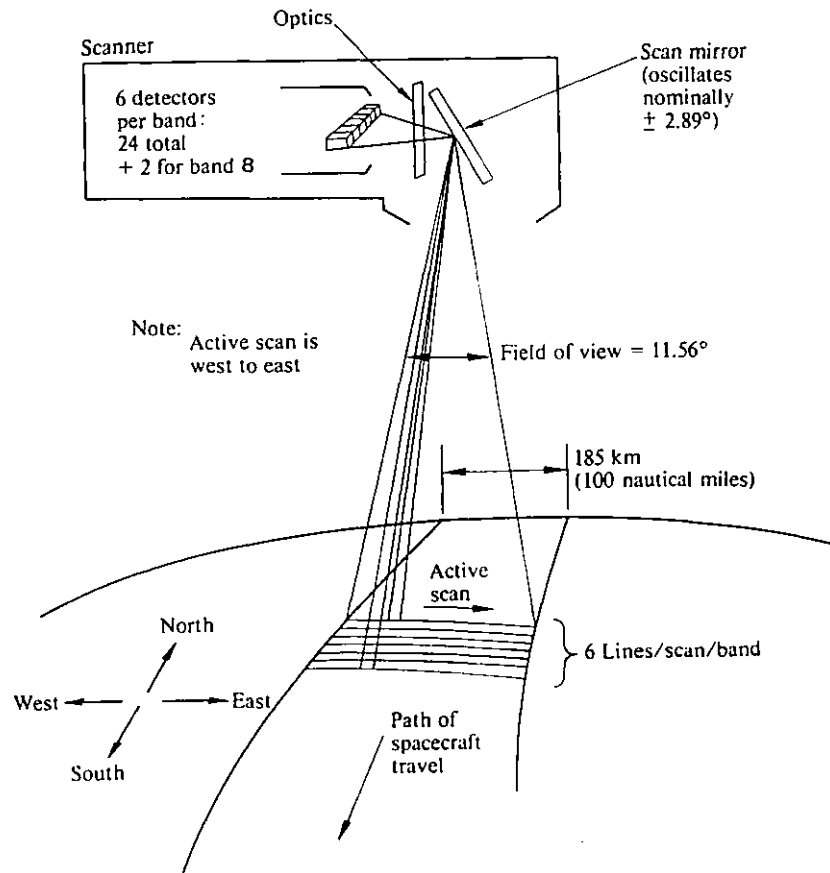
<u>Figure 2.2</u> MSS scanning arrangement (after USGS, 1979).

Band	Spectral Response (Micrometers)	Type of Radiation
4	0.5 - 0.6	Visible, green-yellow
5	0.6 - 0.7	Visible, orange-red
6	0.7 - 0.8	Invisible, near infrared
7	0.8 - 1.1	Invisible, near infrared
8	10.4 - 12.6 (Landsat 3 only)	Invisible, thermal infrared

<u>Table 2.1</u>   MSS spectral response.

The MSS scans six lines of data at a time in the cross-track direction with the forward motion of the satellite providing the along track progression of the scan lines. Since the satellite moves south as the six lines are scanned and the mirror retraces, the scan lines are not quite perpendicular to the pathline (Fig. 2.3). The mirror
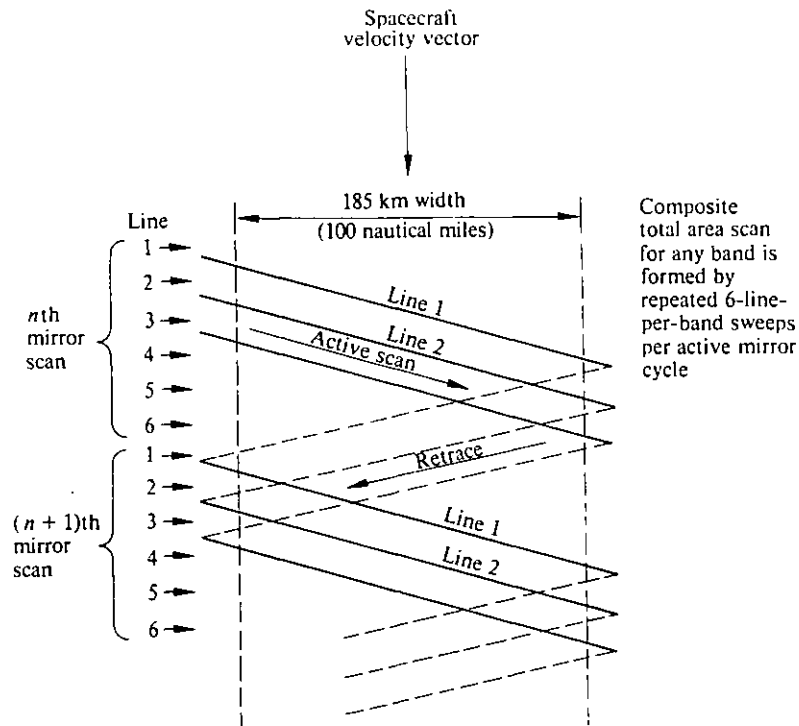
Figure 2.3 MSS ground scan pattern for three of the six detectors in a band (after USGS, 1979).

scan and retrace periods are each 36.71 milliseconds, but scene data are acquired only during 33 milliseconds and an entire four band image in just about 25 seconds. As the mirror scans the earth from west to east the radiation coming from the ground is sampled sequentially by each detector of the array of detectors of the four spectral bands. The sampling sequence causes a minute time delay in the acquisition of data between the four bands and results

in a displacement between these bands. This displacement is corrected during ground processing by the insertion of synthetic pixels, ensuring spatial matching between the bands (Gordon, 1980). During the retrace cycle of the mirror, a shutter blocks off radiation from the earth and the detectors are exposed to internal and sun calibration sources, producing calibration data that are subsequently utilised to make radiometric corrections on the MSS data.

2.3.3.2 Spatial Resolution of MSS Imagery and Pixel Dimensions

The spatial resolution, or resolving power, of an image expresses the minimum size of objects on the ground that can be detected or identified. The measure of spatial resolution most widely used for the MSS is the instantaneous field of view (IFOV). The MSS nominal IFOV is 79m square as determined by the nominal altitude of the satellite, the focal length of the optical system and the detector size. Slater (1979) points out that due to cladding around the optical fibres which transfer the radiance to the detectors, the detector size is reduced and this results in an IFOV of 76.2m square at a nominal altitude of 918.6 km. However, since the altitude of the satellite varies between 880 and 940 km (Taranik, 1977) due to noncircularity of the orbit and nonsphericity of the earth, the 79m IFOV may vary from 76m to 81m (Gordon, 1980).

As the MSS scans the earth from west to east, the voltage produced by each detector is sampled every 9.95

microseconds, resulting in approximately 3,300 samples along a scan line. This rate of sampling causes the nominal ground projected IFOV to move a distance close to 56m on the ground between each sample (Fig. 2.4).

MSS IFOV   Sampling interval of MSS   MSS Picture Element
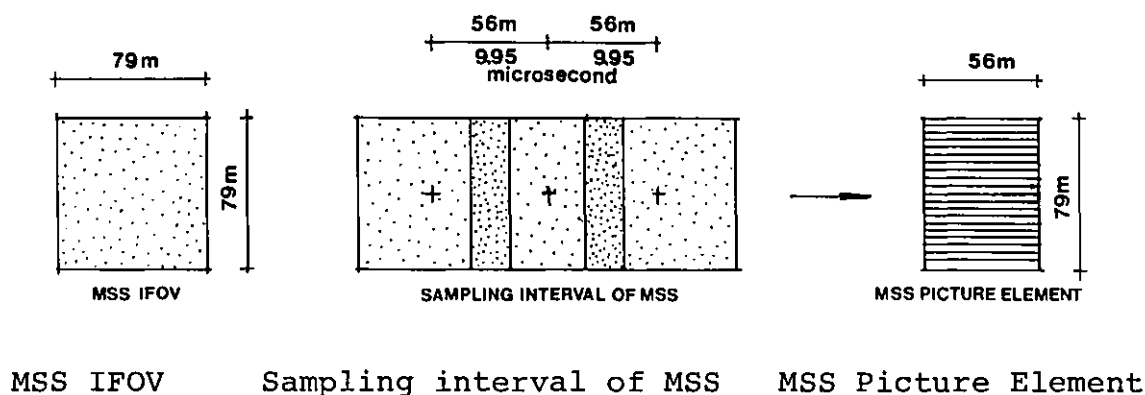
Figure 2.4 MSS sampling interval and picture
element (after Taranik, 1977).

Although the radiation measurement is made from an area of 79 by 79m plus the surrounding area included by the spread function of the optics, this measurement is assigned to an area of 56 by 79m. The 56 by 79m area which is subsequently recorded on a computer compatible tape is called a Landsat MSS picture element or pixel. The oversampling in the scan direction was designed to improve the spatial resolution in that direction, whereas other system design considerations precluded its use in the path direction of Landsat.

2.3.3.3 MSS Imagery Quality

Measures of spatial resolution such as the IFOV has been used to assess imagery quality and judge its potential

applications. However, spatial resolution alone may not always give a true indication of the information content and usefulness of an MSS image since a number of other factors affect the detectability of ground features. Townshend (1981a) discusses these factors which include the contrast between the brightness of the feature and its surroundings, the orientation of the feature in relation to the scan lines, the signal-to-noise ratio of the detectors, the sensor sampling rate, the digitisation process, optical image degradation, and atmospheric effects.

Apparently, the single most important factor is the contrast of the feature with its background. Because the MSS integrates the radiance within the ground area covered by the IFOV, features like roads or rivers which are smaller than the IFOV can be detected if they are sufficiently brighter or darker to change the overall value of the pixel. On the other hand, objects the same size or slightly larger than the IFOV might not be detected if they have a low contrast with their surroundings and the IFOV does not cover it or most of it. Moreover, due to the multispectral character of the MSS images, features detected in one band may not be detected in another band. Thus, detectability can vary all over the image and from band to band.

Other important factor is atmospheric effects which will tend to reduce the contrast of an image and, hence, its chances of detection. Furthermore, detectability can be affected by sensor caused defects such as variations in the

response of the MSS detectors, resulting in image striping. Digital image processing techniques can be used to remove image striping and correct for atmospheric effects (Moik, 1980), improving detectability and, hence, image information content and quality.

Spatial resolution is a valid measure of image quality because it gives an indication of the order of magnitude of the smallest object which can be detected, but it has limitations since it varies according to a number of factors. Therefore, the assessment of the quality of a given MSS image and its usefulness for a specific application should not be based on its spatial resolution alone, but should also take into account its information content which will depend on the multispectral characteristics and variability of the ground features being studied, the performance of the sensor and the atmospheric effects, as well as on the digital image processing techniques applied.

2.3.4 MSS Data Products

The remote sensing data gathered by the MSS sensors are available as digital products in computer compatible tapes (CCTs) and as photographic products in positive transparencies and paper prints from the EROS Data Center, Sioux Falls, South Dakota, and from the other distribution centres around the world. The distribution centre for the United Kingdom is the Remote Sensing Unit of the Space Department, Royal Aircraft Establishment (RAE), Farnborough,

Hants., which disseminates the Landsat data received by the ground stations at Fucino in Italy and at Kiruna in Sweden.

The CCTs provided by RAE can contain the raw data or data that has been radiometrically and geometrically corrected. Special digital products which have been enhanced by various image processing algorithms are also available. The photographic products are recorded on 240 mm first generation films by a Linoscan 204D and contain data which has been radiometrically and geometrically corrected, and contrast stretched. From these masters, positive transparencies and paper prints in black and white and in colour composites are generated (RAE, undated).

The CCTs used in the present study have been corrected radiometrically for variations in the detectors response and geometrically for skewing due to earth rotation under the satellite path. The data are written in an eight bit byte mode, allowing the pixel values to range from zero to 255. However, not all of these values are possible since the original data digitised on board the satellite range from zero to 63 (six bit byte mode).

CHAPTER THREE

LANDSAT IMAGE PROCESSING AND INTERPRETATION

3.1   INTRODUCTION

Image processing encompasses all the various operations performed upon an image in order to optimise the extraction of information and hence to aid image interpretation, which involves the detection and recognition of elements or characteristics of the earth's surface registered on an image and their classification.

Image processing can be implemented in either analogue (continuous signal) or digital (discrete signal) form. In the present study, digital processing was used throughout and performed on an I²S System 500 Digital Image Processing System utilising MSS digital image data contained in computer compatible tapes (CCTs). The I²S System 500, which consists of a Model 70/F4 image processing computer and a System 500 (version 2.3) image operating system and applications program package, is supported by a PDP-11/24 minicomputer. The CCT data was input through a tape interface unit and stored in the minicomputer disc unit. The results of image processing were displayed on a Mitsubishi 19 inches high resolution colour display monitor, which was photographed using a fixed-mounted 35 mm camera.

Digital processing was chosen for the following reasons: first, the MSS image data is inherently digital as

the output of the sensor on board the satellite is digital, so the data can be fed directly into the computer without conversions, preserving the original data precision and avoiding the losses in radiometric detail and spatial resolution associated with the photographic process, and hence providing the most faithful rendition of an image; second, images in digital form can be interpreted at much larger scales than in photographic form and so are specially suited to study geobotanical anomalies which are normally small in size; and third, the speed, accuracy and flexibility of computers to carry out linear and non-linear operations and interactive processes.

A digital image can be described as a two dimensional array of integer values that correspond to discrete measurements of the spectral radiance of an area. Each point of this matrix is called a picture element, or pixel for short. Some processing techniques modify the value of each pixel independently of the value of surrounding pixels and are called point operations whereas others take into account the value of the surrounding pixels and are called local operations (Steiner and Salerno, 1975).

Image processing can be divided, according to its purpose, into three categories: image correction, enhancement, and classification.

3.2   IMAGE CORRECTION

Image correction techniques, sometimes designated as preprocessing, are concerned with the correction for radiometric and geometric distortions induced by the scanning, transmission and recording processes, and by the atmospheric effects. This involves operations such as noise removal and corrections for atmospheric scattering, striping and scan skew. In addition, image correction involves transformations of the original data such as resampling the image to selected cartographic projections, mosaicking, rotations, and reduction and expansion of image scale. The aim is to create a more accurate rendition of the original scene in terms of its radiometric and geometric properties and prepare the image for display, enhancement and analysis.

The CCTs containing the MSS digital image data used in this study have been produced from image data that were geometrically corrected for scan skew due to the rotation of the earth under the satellite path and radiometrically corrected for variations in the detectors response which causes image striping. However, as Taranik (1977) points out, this radiometric correction is seldom perfect and residual striping remains.

The image correction operations performed on the images during this research had the following sequence:

(1)   After selecting in the images the sections containing the area under study at full resolution and registering them, the noise present (pixel and line tape

recording dropouts) was removed using a one-dimensional Tukey median filter.

(2)   The images were then destriped by matching detector means and variances; this is an important step in preparing the image for enhancement because the striping, if not removed, is often also enhanced and may become unacceptable in ratio images (Moik, 1980).

(3)   The images were magnified in order to better display the area of study, since it is small in size, and to be able to analyse the individual pixels. The method of resampling used was nearest neighbour; although it produces images with blocky appearance, this method was chosen because of its computational simplicity and, specially, for its preservation of the pixel values.

Although algorithms for the correction of atmospheric scattering, which affects more strongly the shorter wavelengths and is often called haze, have been developed (Chavez, 1975), it was not performed on the images because the writer agrees with Lillesand and Kiefer (1979) in that the effect of haze is also decreased, so far as the visual appearance of the image is concerned, when a contrast stretch, an enhancement technique, is performed on the image.

3.3   IMAGE ENHANCEMENT

Image enhancement consists of transformations and

manipulations of the image data aiming at aiding the human interpreter with the extraction of information for direct interpretation. Human interpreters commonly extract information from an image by visually detecting and analysing differences in tone or colour, texture, and pattern between the objects depicted in an image. Thus, by increasing the contrast and enhancing colours, texture, and patterns, certain objects or features of interest that may not have been readily apparent in the original image may then be detected and recognized. Hence, the quantity of information extractable from the image is increased, facilitating its interpretation. Although image enhancement places an emphasis on human interpretation, an enhanced image can be used as input to computer image classification (Goetz and Billingsley, 1974).

There are many enhancement algorithms that have been successfully used to aid interpretation from Landsat images for a variety of earth's resources studies. Some of the techniques, apart from enhancing the image, have the advantage of reducing the dimensionality of the data to be interpreted to manageable proportions as it is the case of multi-image enhancements which combine two or more images. A detailed description of these techniques and examples of successful applications can be found in Moik (1980), Townshend (1981b), Sabins (1978) and Gillespie (1980). A brief description of the techniques which were available for application in the present work is given below.

(1)   Contrast Stretching: consists of grey scale transformations applied to the entire image to stretch the contrast in order to fill the dynamic range of the display device and so give a better range of tones between black and white for analysis; the transformations applied to the grey scale histogram of the image can be linear or non-linear (logarithmic, gaussian, histogram equalisation, etc.).

(2)   Additive Colour Composition: is the combination of three images where the corresponding pixels between each of them are assigned to the three primary colours. Its usefulness is due to the fact that the human eye has a much greater ability to discriminate colours than grey tones; normally, the input images are enhanced by other methods before composition (contrast stretched, ratioed, etc.).

(3)   Density Slice: is a method of enhancement which displays a grey level or a range of grey levels of a black and white image as a specific colour; it can also be used as a simple form of classification.

(4)   Pseudocolour: it is a colour enhancement that consists of mapping an entire black and white image into different colours according to the brightness of the pixels.

(5)   Ratioing: is the division of the corresponding pixel values of one image by those of another in order to enhance subtle contrast differences.

(6)   <u>Addition and Subtraction</u>: are multi-image enhancements where the pixel values of one image are added to or subtracted from the corresponding pixel values of another; temporal changes or spectral differences may be enhanced in this way.

(7)   <u>Spatial Filtering</u>: it is an operation that changes the pixel values as a function of the values of surrounding pixels; it filters the image using a convolution filter that emphasises high spatial frequencies (rapid tone changes over a few pixels) or suppresses the low frequencies, thus sharpening the image and enhancing tone differences.

(8)   <u>Transformation to Principal Components</u>: this is a technique used to reduce the number of components (bands) of multispectral images for multi-image enhancements by applying linear transformations to the original data that provides a new set of principal components which are uncorrelated and have the variance of the data condensed into a few of them.

The image enhancement best suited to a specific image vary (Goetz et al., 1975) and the diversity of available methods inhibits generalisations concerning their utility (Townshend, 1981b), therefore the approach to image enhancement in this study has been to consider every type of enhancement as potentially useful and hence all the available methods were experimented on the images. The

extent to which they were useful is evaluated and included in the discussion of results (section 5.8).

3.4   IMAGE CLASSIFICATION

Classification is the process which leads to points or parts of an image being assigned to one of a set of classes. Classification can be achieved by human interpretation through the analysis of tone or colour, texture, and patterns or by computer-aided techniques which use the pixel values in the four spectral bands to classify the image. Swain (1978), Lillesand and Kiefer (1979), Moik (1980), and Townshend (1981b) give a detailed description of computer-aided classification techniques.

Computer-aided techniques are divided in two types: unsupervised and supervised. Unsupervised techniques use only the statistical properties of the image data (pixel values) to establish boundaries between sets of data which naturally cluster and for that reason it is also called clustering. Supervised techniques use training samples of the image data which represent areas of known ground conditions to establish the spectral characteristics of the classes.

Although computer-aided classification techniques have been used successfully in many Landsat earth resources studies, its usefulness is reduced by the fact that the development of classification algorithms, as Hoffer (1978) points out, has not advanced to the point where spatial features (texture and patterns) can be utilised as

effectively as spectral features (tone or colour). Therefore, in the context of this work, an emphasis has been placed in enhancing the image for human interpretation and classification, thus combining the efficiency of enhancement techniques to increase image quality with the human interpreter skills to visually analyse and recognise spatial features, and its capacity to associate and use contextual information. However, computer classification was undertaken and its results are evaluated in the discussion of results (section 5.8).

CHAPTER FOUR

REMOTE SENSING OF GEOBOTANICAL ANOMALIES

3.1   INTRODUCTION

The use of vegetation as a guide to mineralisation has evolved two different methodologies: biogeochemistry and geobotany. Biogeochemistry involves the chemical analysis of plant matter or humus in order to obtain evidence of mineralization in the substrate. In contrast, geobotany is the visual observation of changes in plant morphology and distribution of species related to hidden mineral deposits. The principle underlying the use of plants as a guide to mineralizations is the ability of plants to absorb and to be affected by high concentrations of metals from ore deposits at depth or from a mineralised halo surrounding the ore. Geobotanical methods of exploration have been used for many centuries, whereas biogeochemical methods have only been used since the later 1930s since they depend on the existence of reliable methods of trace element analysis (Brooks, 1972). Although these methodologies differ in scope and application, they complement each other. For instance, biogeochemical techniques can be used to determine the metal uptake by vegetation and establish if the observed signs of plant stress are due to metal stress since other factors such as water stress, nutrient deficiency, salinity, etc., can also cause similar effects (Myers, 1970). On the other hand, once reliable geobotanical indicators of metal stress have been determined after an orientation survey, their

application can reduce and even dispense with the use of biogeochemical survey, thus reducing the costs and time to explore a given area.

The remote sensing of geobotanical anomalies is an obvious mean of further reducing the costs and time of surveying large areas or reaching areas of difficult access once reliable methods of interpretation have been developed. The remote sensing of geobotanical anomalies is based on the fact that metal stressed plants have different spectral reflectance from unaffected plants according to remote sensing studies performed in the natural environment and in laboratory conditions. Apparently, the first successful application of remote sensing to identify and map geobotanical anomalies was undertaken in the later 1920s in Zaire and Zimbabwe when panchromatic aerial photography was used in the search for open spots or vegetation clearings in the bush resulting from high concentrations of copper in the soil, which led to the discovery of copper deposits (Walker, 1929). Despite this early success, the potential of remote sensing to detect vegetation anomalies for mineral exploration was only recognised during the 1960s and especially the 1970s when multispectral aerial photography and satellite imagery became widely available. During these two decades, the research in biogeochemistry and geobotany has been very active and works such as Cannon (1960a), Malyuga (1964), NASA (1968), Brooks (1972) and Rose et al. (1979) have provided a better understanding of the problems involved. At the same time, work on the physical and physiological basis for reflectance changes on vegetation

has been undertaken and many examples of geobotanical remote sensing studies at various levels from many parts of the world have been cited in the literature.

These developments, which are reviewed in this chapter, have led to a growing awareness of the possibility of using remote sensing techniques to detect geobotanical anomalies as an effective tool for mineral exploration.

4.2   BIOGEOCHEMISTRY

According to Malyuga (1964), the science of biogeochemistry has its origins in the early 1930s when the geochemist V.M. Goldschmidt observed that the humus of some forest soils was enriched in most of the minor elements. Hence, he deduced that the plants from which the humus was derived must be correspondingly enriched in these elements and suggested that the analysis of plant material might be an effective method of prospecting. The biogeochemical methods of prospecting were first used by S.M. Tkalich in 1938 when he found that the vegetation could be used to delineate a Siberian iron orebody. However, it was Vernadsky, also a geochemist, who later developed the methods and coined the term biogeochemistry.

Biogeochemistry became a major prospecting tool in the U.S.S.R. and, according to Cannon (1960a), since 1945 an expert in this field has been included on all major geological expeditions and in 1955 the Russian Ministry of Geology and Conservation made biogeochemical work a

mandatory part of all geological exploration programmes. Brooks (1972) has pointed out the predominance of the Soviet Union in this field of research when he made a compilation of the bibliography which shows that 62% of the papers in biogeochemistry were published in Russian. Outside the Soviet Union, the research in this field has been concentrated mainly in Canada, United States, Australasia and Scandinavia.

Analysis of the accumulation of elements in vegetation and the upper humus layer of soils is the basis of biogeochemistry. The mechanisms whereby plants accumulate trace elements are complex but in essence involve uptake via the root system, the passage of the elements through the aerial parts of plants into organs such as the leaves and flowers, and finally a return of these elements to the upper layers of the soil when the leaves or flowers whither and fall. The elements are then leached through the various soil horizons and are reaccumulated by vegetation in a series of steps known as the biogeochemical cycle (Fig. 4.1).

The formation of biogeochemical anomalies, i.e., areas where the vegetation contains an abnormally high concentration of metals, depends on many factors. Ideally, the metal content of vegetation should have a high correlation with the metal content of the substrate. However, the factors discussed below influence this correlation, affecting the reliability of the method and hence should be taken into account if biogeochemical prospecting is to be used efficiently.
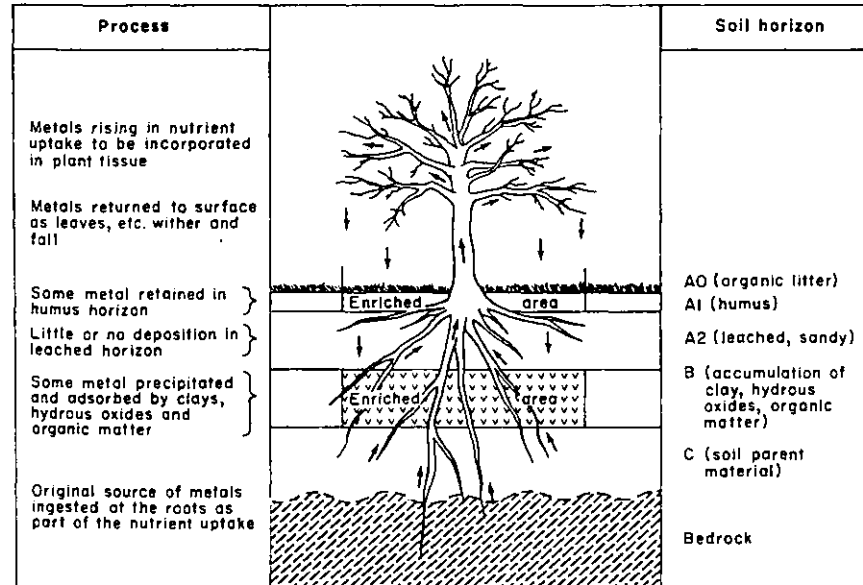
Figure 4.1 The Biogeochemical Cycle. From Rose et al. (1979).

Availability of metals in the soil has been always regarded as the principal factor for biogeochemical anomalies formation. Availability is influenced by the form in which the metals are in the soil, such as free ions, complex ions, ions adsorbed on clay minerals or other colloidal particles, organic complexes, and either primary or secondary minerals (Mortvedt et al., 1972). The forms which can be considered available and absorbed by the plant directly are the free ions, weakly adsorbed ions and some of the inorganic and organic complexes. Soil pH also strongly affects the metal uptake by plants. A decrease in zinc uptake in alkaline soils has been reported by Robinson et al. (1947) whereas Aldrich and Turrel (1951) have shown an increased availability of this metal in acid soils. Press (1974a) reports the same conclusion and notes that only under low pH conditions are the metals in the soil released for uptake by the vegetation. However, the surface of the

root tip and its vicinity shows a relatively high acidity when compared to the soil as a whole. It has been observed that this local acidity can extract metals well in excess of what is readily available and Lovering (1959) points out that even primary silicate minerals can be broken down and made available to the plant.

Another factor which influences the metal content of vegetation is the nutritive requirements of plants. The nutrients required by plants can be included into two categories: macronutrients and micronutrients. Macronutrients are essential elements that are needed in large quantities and which include elements such as C, H, O, N, K, P, S, Ca, and Mg, whereas micronutrients are trace elements which are also important for plant growth but required only in small quantities and include elements such as B, Cl, Cu, Fe, Zn, Mo and Mn (Brooks, 1972). All plants have a different range of requirement for both categories of nutrients, and Rose et al. (1979) points out that different plant species all supported by identical nutrient solutions will contain varying concentrations of many of the trace elements. Thus, when analysing the metal content of vegetation only intraspecies comparisons should be made. Cannon (1960a) have shown this differential uptake by examining the average amount of five general types of vegetation growing in uncontaminated soils (Table 4.1).

The success of biogeochemical prospecting depends to a large extent on identifying and assaying plant species which are highly informative, i.e. plant species which show

Table 4.1 Average metal content (ppm) in the ash of five types of vegetation growing in unmineralised ground. Figures in parentheses show the number of analyses used in the calculations. From Cannon (1960a).

Element	Grasses (above ground)		Other herbs (above ground)		Shrubs (leaves)		Deciduous trees (leaves)		Conifers (needles)		Averages and totals	
Cr	19	(30)	10	(139)	14	(67)	5	(100)	8	(120)	9	(462)
Co	10	(30)	11	(192)	10	(70)	5	(101)	<7	(119)	9	(512)
Ni	54	(28)	33	(226)	91	(182)	87	(209)	57	(213)	65	(858)
Cu	119	(102)	118	(429)	223	(853)	249	(293)	133	(370)	183	(2047)
Zn	850	(62)	666	(355)	1585	(735)	2303	(278)	1127	(333)	1400	(1763)
Mo	34	(32)	19	(217)	15	(104)	7	(118)	5	(145)	13	(616)
Pb	33	(29)	44	(311)	85	(877)	54	(339)	75	(352)	70	(1908)
V	25	(4)	23.5	(39)	25	(6)	16	(14)	21	(77)	22	(180)

a degree of accumulation of the metal being sought that is in direct proportion to the concentration of the element in the soil. The degree of accumulation is affected by physiological barriers, also called metal tolerance, which are variable for different species and limit the uptake of metals when they are highly concentrated in the nutritive medium. Antonovics et al. (1971) reviewed the studies of metal tolerance and the mechanisms whereby plants limit their absorption of excessive quantities of metals, and Kovalevsky (1978) classified plants according to their resistance to metal uptake in "barrier" and "barrier free". Barrier free species are clearly the best for biogeochemical prospecting since they can provide quantitative information about the concentration of metals in the substrate, whereas the barrier type, depending on their barrier characteristics

or degree of metal tolerance, can only provide near-quantitative at high concentrations of metals in the soil and qualitative, and in some cases even lack prospecting informativeness and hence are unsuitable for prospecting. Table 4.2 illustrates this varying degree of metal uptake by different species coming from the same contaminated area.

Table 4.2   Average values for the more common species growing on calamine soils.   From W. Ernest (1965), in Antonovics et al. (1971).

Plant species	Zinc content in ppm dry weight	Number of sites investigated
Thlaspi alpestre ssp. calaminaria	7757	7
Armeria maritima ssp. halleri	3328	5
Minuartia verna ssp. hercynica	3007	17
Silene cucubalus (= vulgaris) var. humilis	1719	27
Armeria maritima ssp. calaminaria	1895	2
Viola calaminaria	686	4

Just as with plant species, plant organs can have different amounts of the same metal. This is due to the fact that the translocation of elements to the upper parts of the plants is selectively controlled in such a way that some elements are freely admitted while others are impeded. Warren and Delavault (1949) have found this difference between plant organs and concluded that leaves usually have higher concentrations of metals when compared to other organs, a fact which was confirmed later by the work of

Brooks (1972) who adds that high concentrations of a specific element in a particular organ do not necessarily imply that this is the best organ to sample and, possibly, an organ with a lower metal content may give a more reliable correlation with the soil concentrations for the element being prospected. Warren et al. (1955) reported that second year twigs gave the most satisfactory results and emphasised that the metal content of plant parts change with age, and hence only organs of the same age should be compared. On the other hand, Kovalevsky (1978) found that the bark of various trees produced good results for most of the elements studied.

The above facts underline the need to conduct an orientation survey of the prospecting area before starting the sampling program, since the identification and use of not all but only highly informative plant species and parts are an important factor for effective biogeochemical prospecting. Once the selection of plant species and parts has been made, sampling should take place over a short period of time in order to minimise the effect of seasonal fluctuations of the plant's metal content which are more significant in leaves and overground parts of grasses than in slowly metabolising or dormant tissues such as twigs, branches, trunks and barks (Brooks, 1973; Kovalevsky, 1978).

Other factors such as climate, soil drainage, and aspect can cause variations in the availability of metals in the soil and in their uptake by vegetation (Malyuga, 1964;

Brooks, 1972; Rose et al., 1979). Although their influence is not so marked, Brooks (1972) recommends that they should be taken into account and any apparent anomalies related to changes in these factors should be examined with care to avoid misleading results.

Despite the numerous factors which can affect the reliability of biogeochemical prospecting, many studies have shown that it is still possible to apply the technique successfully. The reason for this might be that many of the factors discussed above have a minor effect, though in some areas they can be more important than in others, and the overriding factor is the high metal concentration in the nutritive medium of plants. Additionally, through the effort of many researchers in this field, certain procedures have been developed that can reduce or even eliminate the effects of these factors. These procedures which have been listed by Brooks (1972) include: selection by orientation survey of plant species, organs and age of organs; use of ratios of two elemental concentrations; selection of healthy specimens only; avoidance of poorly drained or shady areas if possible; and carrying out work over a short period of time.

Perhaps, the main advantage of biogeochemistry is that a given plant can sample large amounts of ground both vertically and horizontally and hence represent a much larger area than a given soil sample. Biogeochemistry can be a particularly useful technique where trees and shrubs with long root systems may penetrate a nonmineralised overburden, sample closer to the bedrock mineralisation, and under favourable conditions locate concealed orebodies (Cole and Le Roex, 1978; Leavitt and Goodell, 1979).

The biochemical technique has been of value in the present study, for the biogeochemical data available over the Shipham area show the vegetation's anomalous level of metal content and its seasonal variation in metal content, which has established the geobotanical character of certain anomalies observed on the vegetation and provided reference data to the present study of these anomalies by multi-date Landsat images.

4.3   GEOBOTANY

Most plants require small quantities of metals for healthy growth, however when these metals occur in abnormal concentrations in the soil and are available for absorption by plant roots, they may be highly toxic to those species unable to reduce their uptake, thus causing disturbances in the metabolism and development of plants which results in morphological changes and influences the distribution of certain species. Geobotany is the visual observation of vegetation in order to detect anomalies in plant morphology and distribution of species as a guide to ore deposits. Unlike biogeochemistry, geobotany has been used for centuries and the ancient prospectors were well aware of metal uptake and its physiological effect on plants (Cannon, 1979).

In geobotanical prospecting, three aspects of vegetation cover are of significance: the characteristics and distribution of individual indicator plants, the

characteristics and distribution of anomalous plant communities, and the morphological changes observed on plants.

Indicator plants are those species or varieties of plants whose presence and distribution indicates a certain type of mineralisation, rock, or condition in the substrate such as the above average content of metals found in soils over ore deposits or old mineworkings. Indicator plants grow on these soils either because their growth is promoted by the unusual content of metals or because they are tolerant to conditions in which other species cannot survive. Many authors have compiled tables containing the plant species that have been used as indicator around the world (Cannon, 1960; Malyuga, 1964; Antonovics et al. 1971; and Brooks 1972, 1979). In a review of the role of indicator plants in geobotany, Brooks (1979) points out that indicator plants are herbs rather than trees or shrubs and notes that over a third of all indicator plants belong to the families Caryophyllaceae (pink family), Labiatae (mint family), and Leguminosae (pea family).

Indicator plants have been classified by Nesvetaylova (1961), into universal and local indicators. According to Brooks (1972), universal indicators are species which will not grow in nonmineralised substrates and which can be used as indicators in any region in which they occur, whereas local indicators are species adapted to tolerating mineralised ground but which will also grow elsewhere, providing the competition from other species is not too great.

Universal indicators can be extremely useful in prospecting since they are precise indicators of high soil concentrations of the element being sought. Examples of universal indicators include _Thlaspi calaminare_ and _Viola calaminaria_ which only grow on soils with anomalous Zn content. However, they present some problems in their utilisation which stem from the fact that there is only a small number of known reliable universal indicators and their distribution is very limited. Despite these disadvantages, Brooks (1972) states that the greatest successes in geobotany have been obtained with the aid of such species and quotes as examples the discovery of copper in Zambia by use of _Becium homblei_, as reported by Horizon (1959), and uranium by use of _Astragalus_ in the Colorado Plateau, as reported by Cannon (1957, 1960b). Local indicator species are more numerous than universal since they are common, widely distributed species that also grow on mineralised soils but have the disadvantage that their role as indicators of mineralisation in geobotanical prospecting is restricted to a local situation.

The use of plant indicators in geobotanical prospecting is somewhat complicated by the fact that it is sometimes difficult to establish if the distribution of a specific plant is controlled by the element being prospected or by an associated element, as in the case of polymetallic sites, or an environmental factor such as soil pH or water availability. For this reason, Antonovics (1971) comments that the concept of indicator plants is perhaps ecologically unrealistic, although useful as a qualitative assessment.

Nevertheless, once the presence of an indicator has been established in an area, it can be useful in delineating and mapping the location of orebodies and aid the prospecting of other possible mineralisations in the same region, particularly where the underlying mineral deposits are masked by a barren overburden and thus not reflected in soil geochemistry.

The observation and study of the patterns of distribution of species rather than that of a single indicator plant can also aid the recognition and delineation of mineralised ground. Plant communities often serve to identify and map particular lithologies such as limestones or ultrabasic rocks and hence can be useful in mineral exploration because they indicate where certain types of mineralisation are likely to occur (Brooks, 1972). An example of this is the use of anomalies of plant communities associated with ultrabasic rocks for locating chromite deposits (Lyon et al., 1968). The plant communities associated with this lithology are called serpentine floras and show an anomaly in relation to the background vegetation that is characterized by a sparseness of vegetation and a reduced number of species. Cole (1980) has reviewed the use of anomalous plant communities to locate ore deposits and discussed many examples of their successful application in the prospecting of new mineral deposits.

An important aspect of plant distribution in geobotanical prospecting is the existence of bare areas or areas with extremely reduced flora in an otherwise normally

vegetated area. These changes in vegetation density may indicate a deficiency of nutrients or strongly mineralised soils where the toxic effects of metals affect the ecological balance and only species able to adapt to this environment may survive. Vegetation clearings or dambos have been successfully used as a guide to ore deposits in Zambia where some of the big Cu deposits were originally discovered because of this effect (Rose et al., 1979).

In addition to the absence of indicator plants and anomalous plant communities, another type of geobotanical anomalies that can be useful aids in prospecting are the morphological changes induced in plants by the toxic effects of metals. These morphological changes include dwarfism, gigantism, and other changes in form of either the whole or parts of the plant, mottling or yellowing of leaves (chlorosis), changes of colour in flowers, and disturbance in the seasonal rhythm of flowering. Table 4.3 summarises the changes that have been observed in plants due to excess of metals.

These morphological changes, some of which are element specific while others are not, have been extensively and adequately described by Malyuga (1964) and Brooks (1972). The latter author proposes various mechanisms whereby metals can cause morphological changes in plants by their toxic action, the most common being: poisoning of enzymes; replacement and precipitation or immobilisation of essential nutrients, causing nutrient deficiency; catalytic

Table 4.3   Physiological and morphological changes in plants due to metal toxicity. From Cannon (1960a).

Element	Effect
Aluminium	Stubby roots; leaf scorch; mottling.
Boron	Dark foliage; marginal scorch of older leaves at high concentrations; stunted, deformed, shortened internodes; creeping forms; heavy pubescence; increased gall production.
Chromium	Yellow leaves with green veins.
Cobalt	White dead patches on leaves.
Copper	Dead patches on lower leaves from tips; purple stems; chlorotic leaves with green veins; stunted roots; creeping sterile forms in some species.
Iron	Stunted tops; thickened roots; cell division disturbed in algae, resulting in greatly enlarged cells.
Manganese	Chlorotic leaves; stem and petiole lesions; curling and dead areas on leaf margins; distortion of laminae.
Molybdenum	Stunting; yellow-orange coloration.
Nickel	White dead patches on leaves; apetalous sterile forms.
Uranium	Abnormal number of chromosomes in nuclei; unusually shaped fruits; sterile apetalous forms; stalked leaf rosette.
Zinc	Chlorotic leaves with green veins; white dwarfed forms; dead areas on leaf tips; roots stunted.

decomposition of essential nutrients and metabolites; and reduction of cell wall permeability, preventing the free passage of K, Na, and organic molecules. However, Antonovics et al. (1971) point out that metal tolerant plants are metabolically different from normal plants and

that the mechanisms and degree of metal tolerance are specific for each metal, the effect of one metal being different for different plants. Therefore, the presence of morphological changes on the vegetation growing over mineralised substrates will ultimately depend on the degree of metal tolerance of individual plants to the metal concentrated in the soil and its availability for plant uptake, although seasonal effects may play an important role. For instance, the seasonal variations of metal content of aerial parts of plants such as leaves and overground parts of grasses, which are caused by remobilisation of elements within the plant rather than variable uptake (Matthews and Thornton, 1982) may produce periodic morphological changes or make them more apparent when the metal content peaks, reverting to normal when it is reduced.

Chlorosis is the most common symptom of metal toxicity and has been a useful guide to ore deposits. This yellowing of the leaves of plants is nearly always an indication of deficiency of iron necessary in the formation of chlorophyll. Usually, this iron deficiency is not related with low levels of iron in the substrate but rather is a result of the antagonistic effects of excessive amounts of Cr, Co, Cu, Mn, Ni or Zn towards uptake of iron by plants (Brooks, 1972). Therefore, chlorosis cannot indicate the presence of a specific metal in the soil but it can be a useful guide to additional mineralisations in areas of known ore deposits, or at least can indicate that some type of mineralisation may be present. Chlorosis is normally more apparent and widespread during certain times of the year,

probably because of the seasonal variations in plant's metal content mentioned above or eventually to an additional environmental stress such as extremes of climate.

The types of geobotanical anomalies present on the vegetation growing over mineralised soils in Shipham, which consists of grasses and weed species, are the following: the occurrence of Thlaspi calaminare, an indicator plant usually associated with Zn mineralisations (Smith, 1978); the presence of chlorosis, usually during late winter and early spring, and reduced vegetation density including some bare patches (Matthews and Thornton , 1982).

Studies of geobotanical anomalies applied to mineral exploration were usually based on ground surveys carried along line or belt transects, or using quadrats, however the use of remote sensing techniques in geobotanical studies has been increasing, mainly because of its potential for rapid surveying of large areas and low cost. The possibility of studying these anomalies on a seasonal basis without much additional expenditure is another reason for the increasing use of remote sensing data, especially multitemporal Landsat imagery, since seasonal effects seem to play an important role and render some of these anomalies more apparent during certain times of the year.

In general, the types of geobotanical anomalies that can be detected and interpreted by remote sensing depend on the size of the anomaly, its distribution pattern and degree of contrast with the surroundings, as well as on

the image resolution and quality. Obviously, some of the geobotanical anomalies discussed above, particular subtle plant morphological changes, can only be observed on the ground. However, indicator plants and plant communities, bare areas or areas or reduced flora, and chlorosis when widespread, are features that can probably be detected and mapped by aerial imagery and even possibly by satellite imagery.

4.4   REVIEW OF REMOTE SENSING STUDIES OF GEOBOTANICAL ANOMALIES

4.4.1   Introduction

Remote sensing is the collection of information about an object, area or scene from measurements made at some distance from it and related in some way to the earth's natural resources or environment. The effect most frequently measured by remote sensing systems is the electromagnetic energy emanating from the target of interest, although there are other phenomena that can be measured such as electric, magnetic and gravitational forces which have been used in the field of geophysical prospecting.

Remotely sensed data can be acquired by sensors that record radiation in one or more parts of the electromagnetic spectrum and from various levels of altitude or degrees of proximity to the target, thus producing a wide range of remote sensing products in terms of spectral and

spatial resolution. The data collection can be made from platforms such as aircraft and spacecraft or on the ground, whether in the field or laboratory. The remote sensing systems that have normally been used from aircrafts and spacecrafts include imaging systems like photographic cameras, scanners, side-looking airborne radars (SLAR), and passive microwave radiometers, whereas on the ground the most commonly used equipments are non-imaging such as spectroradiometers and spectrophotometers, the latter being confined to laboratory measurements. A detailed description of the various sensor systems can be found in Reeves (1975) and Slater (1980).

The remote sensing systems that have normally been used to study the reflectance of metal stressed vegetation include photographic cameras, scanners, spectroradiometers, and spectrophotometers. Photographic camera systems use films which are sensitive to the region of the spectrum ranging from about 0.4 μm in the visible to about 0.9 μm in the near-infrared (see Fig. 1.1) to record radiation and, through the use of various films and filter combinations, can produce photographic imagery of just one part of this spectral region or several parts of it (multispectral photography) in either black and white or colour. The camera is the oldest and perhaps best known and widely used remote sensing instrument. However, scanners systems that use detectors rather than films are being increasingly applied to acquire remote sensing data because they present some advantages in relation to photographic systems such as the possibility to sense wavebands beyond the visible in a

registered multispectral fashion and, important in the case of unmanned satellites, the ability to transmit the data directly to a ground receiving station where they are recorded on computer compatible tapes and thus can be directly fed into a computer for subsequent image processing, whereas photographic film need to be physically recovered and requires scanning and digitising before computer image processing can be performed. The multispectral scanner (MSS) of the Landsat satellites, probably the best known and most used scanner system, has provided the remote sensing data used in the present study and is described in detail on Chapter 2. Spectroradiometers and spectrophotometers are non-imaging instruments that measure the spectral radiance properties of objects in narrow wavelength intervals through the use of various techniques that disperse the radiation entering the instrument and isolate narrow wavelength intervals. Spectroradiometers use the sun as a source of radiation whereas spectrophotometers are equipped with an internal radiation source.

In the remote sensing studies published in the open literature and reviewed herein, two approaches to the problem of detecting metal stressed vegetation and elucidating its spectral properties have been basically followed. One has been to use high spectral resolution instruments such as spectroradiometers and spectrophotometers to measure the spectral radiation of individual leaves or plants on the ground, thus eliminating much of the interference caused by the atmosphere on the radiation and examining in much greater detail the relationships between the vegetation

characteristics and spectral radiation properties, in an attempt to develop solutions that could be applied to aerial and satellite remote sensing surveys. These ground measurements were conducted either in laboratory controlled experiments where the plants were growing in solutions or soils containing known quantities of metals, or in the field where the natural vegetation was growing on geochemically anomalous soils. The other approach has been to use broad spectral band sensors carried on aircraft and satellite platforms, in order to assess the possibilities of detecting these vegetation anomalies and to develop interpretation methods for their identification that could be used for mineral exploration. The type of energy most commonly used for remote sensing of vegetation metal stress has been the reflected solar radiation, parts of which are sensed by the Landsat MSS. Accordingly, this review will only consider the studies on the region of the electromagnetic spectrum from 0.4 μm to 2.6 μm which include the visible and reflected infrared,

4.4.2   Laboratory and Field Spectral Reflectance Studies of Metal Stressed Vegetation

        In the general field of remote sensing, vegetation is one of the most important targets and a knowledge of how solar radiation interacts with vegetation is necessary to interpret remote sensing data for applications in agriculture, forestry, ecology, and mineral exploration in vegetated terrain. Hence, considerable research has been

undertaken in order to establish the physical and physiological basis for the reflection of visible and reflective infrared radiation in the spectral range 0.4 μm to 2.6 μm, where the incident solar radiation is largely concentrated. The solar radiation incident on a leaf is either absorbed or transmitted, only a part of it being reflected. Figure 4.2 shows the reflectance spectrum of green vegetation and the factors that control it.

In the visible region of the spectrum, pigmentation dominates the spectral response of plants due to high absorption by leaf pigments, especially chlorophylls, although carotenoids, xantophylls and anthocyanins also play a significant role. Therefore reflectance is low in the visible with a peak at about 0.55 μm in the green region, which accounts for the green colour of healthy plants
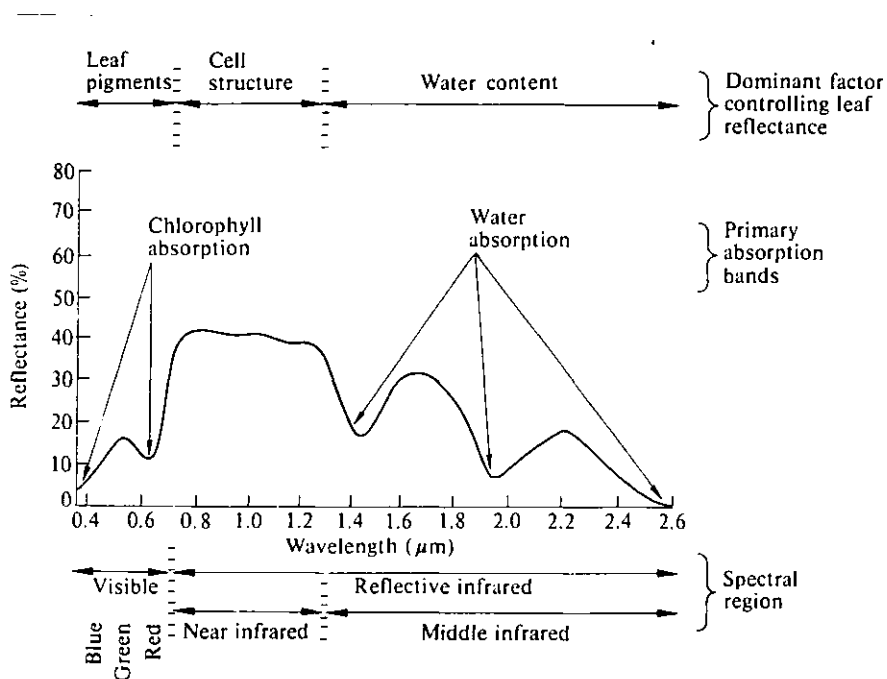
Figure 4.2   Significant spectral response characteristics
              of green leaves.   From Hoffer (1978).

perceived by the human eye. The internal cellular structure is the factor that largely controls the reflectance in the near infrared region from 0.7 μm to 1.3 μm, where the absorption is very low and both reflection and transmission are high due to upward and downward scattering by refractive index discontinuities between intercellular air space and hydrated cell walls. In the middle infrared region from 1.3 μm to 2.6 μm, where the reflectance gradually decreases, the spectral response of leaves is dominated by water absorption bands (Gates et al., 1965; Myers and Allen, 1968; Hoffer and Johannsen, 1969; Gates, 1970; Knipling, 1970; Woolley, 1971; Gausman, 1974).

The typical pattern of spectral response for healthy green leaves shown in Fig. 4.2 suggests that it might be possible to relate reflectance changes in particular regions of the spectrum to changes induced in leaf pigmentation, structure, and water content, by specific physiological disturbances due to metal stress.

Investigations of the spectral response of plants aimed at establishing a relationship between leaf reflectance and metal stress were carried out in the laboratory by Press (1974a,b), Horler et al. (1980), and Chang and Collins (1980), with plants grown under controlled conditions in solutions or soils containing known quantities of metals. These laboratory reflectance measurements, which are free of atmospheric and background noise that affect the data quality, were made on single leaves using a spectrophotometer. The results summarized in Table 4.4 show

a relation of plant metal stress with increased visible reflectance and decreased near infrared reflectance, except for Press (1974a,b) who found no differences between healthy and metal stressed plants in the near infrared region of the spectrum. The increased visible reflectance has been correlated with decreased chlorophyll concentrations caused by metal toxicity. This destruction or lack of synthesis of chlorophyll causes plants to absorb less in the chlorophyll absorption bands and have a higher reflection, particularly in the red portion of the visible spectrum, thus producing visible chlorosis or yellowing of leaves. The decreased near infrared reflectance has not been correlated with any possible changes in leaf cellular structure.

Table 4.4 Summary of reflectance changes in plants grown on mineralised solutions or soils in the laboratory compared to control plants.

Reference	Species	Metals	Effect on Visible Reflectance	Effect on Near Infrared Reflectance
Press (1974a,b)	Beans	Pb,Zn	Increases	No Change
Horler et al. (1980)	Peas	Cu,Cd	Increases	Decreases
	Soybean	Cu,Zn	No data	Decreases
	Sunflower	Cu,Zn	No data	Decreases
Chang and Collins (1980)	Sorghum	Cu,Zn,Ni	Increases	Decreases
	Mustard	Cu,Zn,Ni	Increases	Decreases

Although the reflectance properties of single leaves are important to understand the reflectance of a plant or vegetation canopy, they cannot account for the reflectance of plant canopies in a field situation. The

reason for this is that laboratory measurements using spectrophotometers obtain hemispherical (or total) reflectance data, whereas measurements in the field using spectroradiometers or other imaging sensors obtain bidirectional reflectance data which are variable according to the sun and sensor orientation with respect to the plant canopy. Furthermore, a plant canopy is normally a mixture of different components, including leaves, other plant organs, background, and shadows, all of which influence the radiation reflected by the canopy and recorded by the sensor. Colwell (1974) has reviewed the influence on vegetation canopy reflectance of additional factors other than leaf reflectance which are important in certain situations and have summarised them. They include factors such as leaf area index, leaf orientation, leaf transmittance, reflectance and transmittance of other plant organs, solar illumination angle, sensor viewing angle and azimuth, the amount of shadow, and the amount of background (soil, rock, leaf litter, etc.) viewed by the sensor and its reflectance properties.

Reflectance studies of natural vegetation growing on geochemical anomalous soils, using spectroradiometers which record bidirectional reflectance of plant canopies rather than hemispherical reflectance of single leaves, have provided results which are more meaningful from the remote sensing point of view since they account for the many factors mentioned above that affect the interaction of light with a plant canopy and hence are more reliable to help predict or understand the tone of these vegetation anomalies

on aerial or satellite remote sensing imagery. These in situ measurements were obtained by placing the spectroradiometer in a position above the plant canopy through the use of cherry-pickers or other types of platform, although a vertical viewing angle such as in aircraft or satellite-based sensors was often impossible to achieve. Therefore, according to the field conditions of each investigation, the measurements may have been obtained at differing viewing angles in relation to the plant canopies, a fact which might explain some of the variability observed in the results. The results of these investigations are summarized in Table 4.5. This table shows that, except for Yost (1975) and Howard et al. (1971), an increase has been observed in the reflectance on visible radiation for vegetation growing over mineralisations, compared to surrounding vegetation.

Horler et al. (1980) have suggested that the conflicting results of visible reflectance obtained by Yost (1975) might be due to the possibility of the plants not being affected by the mineralisation since there is no clear evidence that their roots were sampling the orebody, which is covered by overburden and was not detected in geochemical soil analysis. Furthermore, Howard et al. (1971) in the discussion of their own results, commented that a number of important factors may account for the lack of effect on the visible reflectance of plants growing on metal contaminated soils that has been observed in their study, including seasonal variations.

Table 4.5 Summary of reflectance changes of vegetation growing on mineralized terrain, compared to surrounding vegetation not affected by mineralisation. The reflectance measurements were carried out in the field using spectroradiometers, except for Birnie and Dykstra (1978) and Collins and Chiu (1979) where the spectroradiometers were airborne.

Reference	Species	Metal	Effect on Visible Reflectance	Effect on Near Infrared Reflectance
Howard et al. (1971)	Pinus ponderosa	Cu	No effect	Increases
Canney et al. (1971)	Picea rubens	Cu,Mo	Increases	Decreases
	Abies balsamea	Cu,Mo	Increases	Increases
Yost (1971)	Picea rubens	Cu,Mo	Increases	Decreases
	Abies balsamea	Cu,Mo	Increases	Increases
Press (1974a)	Quercus sp.	Pb,Zn	Increases	Decreases
Lyon (1975a)	Pinus monophylla	Mo	No data	Decreases
	Juniperus utahensis	Mo	No data	Increases
Yost (1975)	Pinus ponderosa	Cu	Decreases	Decreases
	Juniperus sp.	Cu	Decreases	Decreases
	Quercus sp.	Cu	Decreases	Decreases
Birnie and Dykstra (1978)	Pinus contorta	Cu,Mo	Increases	Increases
Collins and Chiu (1979)	Conifers	Cu,Pb,Zn	Increases	Increases

This apparent general trend of higher visible reflectance for metal stressed plants is in agreement with the results of laboratory investigations previously discussed, however it should be noted that similar effects have been reported for plants under a variety of stresses such as nutrient deficiency (Thomas et al., 1966; Myers, 1970; Younes et al., 1974), salinity and water deficiency (Ward, 1969), disease (Suits and Safir, 1972), and water

stress (Myers, 1970). This effect on visible reflectance is often associated with chlorosis that is a common symptom of metal stress though non-specific.

The results on the near infrared portion of the spectrum are quite variable and show no apparent trend since an increase in reflectance of metal stressed plants is observed in some cases and in others a decrease. The increases in near infrared reflectance were possibly due to changes in leaf structure that produced an increase in refractive index discontinuities, enhancing radiation scattering and hence reflectance (Knipling, 1969; Wiegand et al., 1972). On the other hand, the decreases could have been induced by a decrease in leaf area index (LAI) due to loss of foliage or plant growth inhibition (Myers, 1970; Knipling, 1970; Colwell, 1974).

The spectrometric investigations reviewed above suggest that the detection of chlorosis offers the best possibilities, although supporting field data to establish whether the observed signs of chlorosis are associated with metal stress or other type of plant stress will be necessary. These investigations were carried out to predict or understand the tone of metal stressed vegetation on remote sensing imagery in relation to the surrounding vegetation, however in addition to the reflectance properties of individual leaves or plant canopies there are other types of information which are also important to the detection of geobotanical anomalies by remote sensing imagery, since the recorded spectral reflectance data

contain a mixture of plant and background information. Thus, depending on the spatial resolution of the image, variations in tone or texture may provide information about the appearance of plants, their cover density and distribution pattern and, hence, aid the identification of vegetational features which could indicate the presence of geobotanical anomalies.

4.4.3   Aircraft and Satellite Remote Sensing Studies of Geobotanical Anomalies

The examples of remote sensing studies of geobotanical anomalies using data obtained by broad-band imaging sensors carried on aircraft and satellite platforms have been concerned with the analysis of images in order to assess the possibilities of detecting these vegetation anomalies and to develop interpretation methods for their identification that could be applied for mineral exploration. In these studies reviewed herein, both visual and computer methods of image analysis have been employed to interpret several types of aerial photographs and satellite images.

An early application of remote sensing to detect geobotanical anomalies for prospecting was carried out in Zaire and Zimbabwe, Central Africa, where panchromatic aerial photography was successfully used to locate open spots in the bush cover due to high concentrations of copper in the soil, leading to the discovery of copper deposits (Walker, 1929). However, it was only until the 1960s and

1970s with the wide availability of new remote sensing techniques and products that the interest in the remote sensing of geobotanical anomalies has increased considerably. Accordingly, NASA published a literature survey assessing the possibilities of applying the new developments in remote sensing technology to study vegetation anomalies induced by mineralisations (NASA, 1968).

Carraro (1973) examined the feasibility of discriminating the Vazante zinc deposits located in the State of Minas Gerais, Brazil, from the background geology. The results showed that it was possible to discriminate the mineralised rocks by their colour response on Aerochrome infrared film at the scales 1:15,000 and 1:30,000. He concluded that this spectral response was due to an anomalous plant community consisting of grasses (Heteropogon villosus, Paspalum trachycoleon, and Axonopus chrysodactus) and a shrub (Gomphrena sp.), which is associated and delineates the mineral deposit.

The work of Cole et al. (1974a) in Africa and Australia have further demonstrated the usefulness of aerial photography in locating geobotanical anomalies. In the Witvlei area of South West Africa, anomalous communities of Helichrysum leptolepia were apparent on black and white aerial photography (1:15,000 scale) as vegetational banding, and follow-up field studies of this anomaly led to the discovery of copper mineralisations in sedimentary rocks. In another area in South West Africa, a geobotanical anomaly

associated with copper mineralisation and characterised by
Dichrostachys cinerea could be detected by a distinctive
dark red colour on colour infrared photos taken with a hand
held camera from an aircraft at a flying height of about
1,500m. In the Mount Isa-Cloncurry area, Western
Queensland, Australia, multispectral photography, colour
photography and colour infrared photography at the scales of
1:5,000 and 1;15,000 were used by Cole et al. (1974b) to
study geobotanical anomalies over the Dugald River lead-zinc
deposit. The geobotanical anomaly which is the surface
expression of the Dugald River deposit is characterized by a
plant community dominated by Eriachne mucronata and
Polycarpea glabra that produced a distinctive spectral
response on all photos, but was most clearly delineated on
infrared colour photography. Further interpretation of
these infrared photographs revealed a number of areas with
similar colouration, which follow-up field investigations
have shown to be geobotanical anomalies associated with
copper mineralisation.

Canney (1975) reported experiments using
multispectral photography in order to detect changes in
vegetation caused by abnormal concentrations of metals in
the soils of two test sites in Montana, USA. In the
Stonewall Mountain site, the infrared band showed a tonal
anomaly which corresponds to the area of copper-lead-zinc
mineralisation, and he concluded that this tonal anomaly was
due to spectral-textural properties of the vegetation that
consists of chlorotic and stunted timber pines. However, no
tonal anomalies were observed over the lead mineralization
in the Elk Creek site.

Further studies of geobotanical anomalies using aerial photography have been conducted by Rosholt (1977) in Norway. The results show that the hill areas of copper poisoned vegetation at Raitevarre, consisting of grasses and an abundance of <u>Viscaria alpina</u> (copper flower) could be detected on black and white photographs. He also used infrared photographs, on which it was possible to delineate the areas with soil copper content greater than 1000 ppm.

In addition to aerial photography, satellite imagery obtained by the Landsat multispectral scanner system (MSS) has also been used to study geobotanical anomalies. Apart from the low price and ready availability, the main advantages of MSS imagery for geobotanical studies are its registered multispectral nature, repetitive cover pattern, and inherent digital format. The advent and growing availability of interactive computer image processing systems have provided the means to process the MSS digital data in a quantitative and reproducible fashion, allowing analyses and interpretation at full resolution and, hence, aiding the full exploitation of the imagery potential for the remote sensing survey of geobotanical anomalies on a multispectral and multitemporal basis. However, the MSS nominal spatial resolution of 79 m appears to be a limitation to its use in the detection of geobotanical anomalies since these features are normally subtle and small in size. Some investigators have reported that the spatial resolution of the MSS imagery proved to be inadequate to their studies (Press, 1974a and b; Cole et al., 1974a and b; Cole, 1977; Talvitie, 1979). Yet, other researchers

were able to apply successfully Landsat MSS digital data to their studies of geobotanical anomalies for mineral exploration.

Levine (1975) used multitemporal Landsat MSS digital data to study an area on the San Francisco Peninsula aiming at detecting serpentine soils. The results show that the serpentine soils could be isolated on the imagery dated 6 October 1972, where it displayed a dark grey tone and was classified by a clustering algorithm. Study of earlier images revealed that this pattern persisted, but with diminishing intensity, until the 26 July 1972 image after which it could not be recognised. He found that this seasonal variation of spectral response was correlated with the dieback and growth cycle of the grass canopy covering these soils.

Lyon (1975b) reports the use of computer enhanced MSS imageries to study five areas, with varying degrees of success. These areas presented increasing vegetation cover density: unvegetated (Yerington and Goldfield, Nevada), moderately vegetated (Pine Nut Mountains, Nevada), and densely vegetated (Karasjok, Norway; and Tifalmin, New Guinea). He found that the increase in vegetation density made the recognition process more complex and geobotanical and biogeochemical field data became essential for the location of these areas. The computer image processing was carried out using an interactive system where the MSS imageries were displayed and manipulated at full resolution, often using only 100 pixels or so. Of the enhancement

techniques employed, ratioing was found to be the most useful. In the moderately vegetated Pine Nut Mountains area, a biogeochemical anomaly (75 to 500 ppm of molybdenum in the juniper and pine needles) was detected on MSS imagery, especially on bands 7/4 ratio which showed the shape and location of the anomaly. In the densely vegetated Karasjok area, Norway, a copper induced geobotanical anomaly in the birch forest was successfully located on MSS imagery, being clearer on band 6.

Further Landsat MSS remote sensing studies at Karasjok by Bolviken et al. (1977) revealed that this copper induced geobotanical anomaly had a low MSS bands 7/5 ratio. The application of a clustering algorithm located further anomalous areas. However, they concluded that although it was possible to locate on the imagery the main copper geobotanical anomaly, the spatial resolution of the MSS was too coarse to identify all the known geobotanically anomalous areas at Karasjok. They pointed out that this problem could be overcome by utilizing remote sensing data obtained from digitized multispectral aerial photography or airborne scanners.

In the Echassieres area, French Massif Central, Lefevre (1980) carried out a multitemporal remote sensing study using MSS digital data. Two vegetation anomalies related to lithium, tungsten, arsenic and tin mineralisations could be located on the images. One of the anomalies in grassland area was apparent on March and April imageries while the other in woodland area was recorded on

June imagery. He concluded that these seasonal anomalies seem to be associated to a particular phenological stage of the vegetation, during the beginning of the chlorophyllian activity and disappear after that.

Darch (1982) also used multitemporal Landsat MSS digital data to carry out a remote sensing geobotanical study. The site was the Dolfrwynog Bog and surrounding Coed y Brenin Forest, North Wales. The Bog supports a copper induced geobotanically anomalous plant community consisted mainly of <u>Armeria maritima</u>, <u>Molinia caerulea</u>, and <u>Festuca ovina</u>. Her results showed that the Bog had a lower reflectance both in the visible and near infrared bands than control sites, being more apparent during spring and early summer when the copper concentration in vegetation peaked and the flowering period started. She suggested that biogeochemical seasonality and phenological stage seemed to contribute to the detection of the Bog and may play an important role in making geobotanical anomalies more apparent at some times of the year.

In conclusion, it seems that the task of locating geobotanical anomalies for mineral exploration through the analysis and interpretation of remote sensing imagery is a complex one due to some limiting factors in biogeochemical, geobotanical, and remote sensing techniques, which include: (a) the possibility that the vegetation growing over a mineralisation has developed some degree of metal tolerance and hence may not be significantly more stressed than the surrounding vegetation in order to produce vegetational

anomalous features or reflectance changes that could be detected by remote sensing; (b) biogeochemical and geobotanical seasonality and phenological stage seem to be important factors and may render a geobotanical anomaly more or less apparent according to the time of the year, thus affecting its detectability; and (c) the spectral and spatial resolution of an image can be significant limiting factors. However their importance will depend on the size of the geobotanical anomaly being studied and its contrast with the surroundings. Nevertheless, the examples of previous remote sensing studies reviewed herein show that it is possible to detect geobotanical anomalies under favourable conditions, though at the present stage it seems difficult to isolate geobotanically anomalous areas without supporting field data. Even though the Landsat MSS imagery has a lower spatial resolution than aerial photography, and a greater signal attenuation due to increased intervening atmospheric path, there is a growing interest in their application to study geobotanical anomalies. This interest can be attributed to some advantages of MSS imagery such as its multi-spectral nature, repetitive cover pattern, synoptic view over large areas, low price, and ready availability, as well as the continuity of the Landsat Programme with future satellites that will provide image data in narrower bands and with increased spatial resolution. The combination of the human interpreter skills with the flexibility, accuracy, and speed of computer systems to carry out image operations seems to offer the greatest potential for discriminating very subtle reflectance differences and abstracting the full information content of Landsat MSS imagery in order to detect geobotanical anomalies as a tool for mineral exploration.

CHAPTER FIVE

REMOTE SENSING STUDY OF THE SHIPHAM TEST SITE

5.1   INTRODUCTION

The test site chosen for this Landsat remote sensing study was Shipham, located on the Mendip Hills, Somerset (Fig. 5.1).

This site has been selected because it is associated with vegetational biogeochemical and geobotanical anomalies induced by a soil geochemical anomaly which is characterised by very high concentrations of Zn, Pb, and Cd due primarily to the underlying lead-zinc mineralisation and secondarily to past mining activities that have ceased in the middle 19th century (Smith, 1978; Goodman, 1979; Matthews and Thornton, 1980). The metal content of the vegetation, consisting of grasses and herb species, has been studied in detail by Matthews and Thornton (1980, 1981, 1982). Their data and the author's own ground observations comprise the reference data used for interpreting the Landsat imagery.

Although the soil geochemical anomaly extends widely over an area of 800 hectares around the village of Shipham, the site of highest metal concentration lying immediately north of the village, whose vegetation show signs of metal stress and so is a geobotanical anomaly, is only about 10 hectares in size. Since each pixel on a Landsat CCT covers an area of 56 by 79m or 0.44 hectares (see Section 2.3.3.2), this site should be represented by approximately 20 pixels.

Lower Langford

A 38

Churchill

Sandford

A 368

A 368

Sandford Wood

Quarry

Mendip
Lodge Wood

Star

Shipham Test Site

Heath

Mendip Forest

Shipham

Winscombe

A 38

Mendip
Hills

Quarry

Kings
Wood

Quarry

Quarry

Rose
Wood

Cheddar
Wood

Quarry

Cheddar Gorge

Axbridge

Cheddar

Cheddar
Reservoir
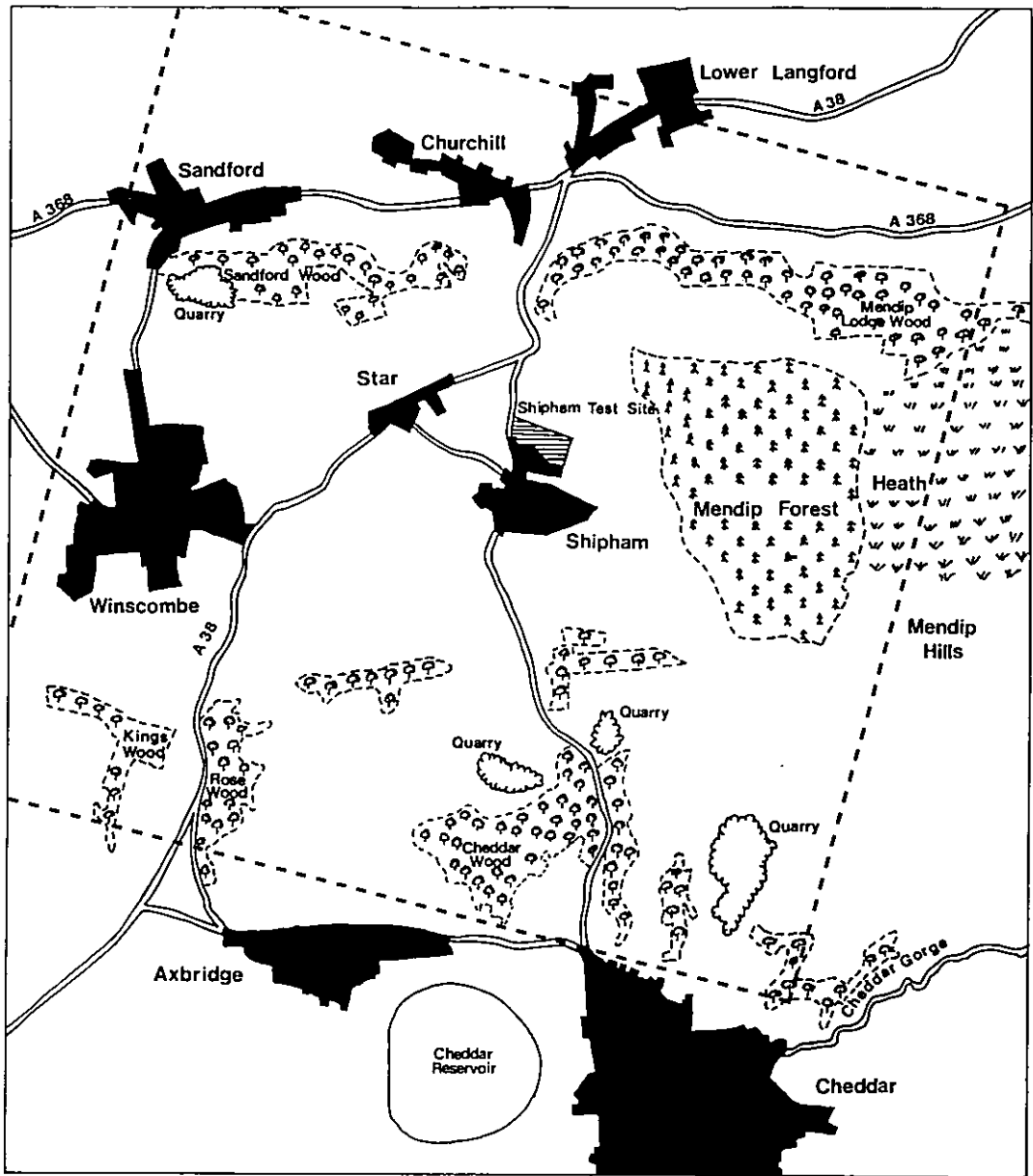
0   1   2
kilometers

Coniferous Woodland

Deciduous Woodland

Heathland

Grassland and Arable Land

Geobotanical Anomaly

Urban or Built-up Land

Quarry

Figure 5.1 Location Map of the Shipham Test Site.

However, due to the occurrence of boundary pixels, the number of pixels that actually depicts only the geobotanical anomaly is reduced to less than this figure. Despite its small size, it was possible to study this site by using digital methods of image processing that allow the analysis and interpretation of Landsat imagery at much larger scales than analog methods.

Three Landsat images were selected and used to conduct the remote sensing study of the Shipham geobotanical anomaly: 27 May 1977, 9 March 1980, and 2 October 1980. The characteristics of Landsat MSS imagery are described in detail in Chapter 2, whereas Chapter 3 outlines the techniques used to process the images, in order to aid the extraction of information by visual interpretation and computer-aided classification.

Before reporting the results of this multitemporal remote sensing study, which aimed at detecting the Shipham geobotanical anomaly and determining its spectral response pattern in relation to the surrounding vegetation, a description of the Shipham test site will be given.

5.2   THE GENERAL GEOLOGY, MINERALISATION AND PAST MINING
       ACTIVITY

The Shipham test site lies on the core of the Blackdown pericline which is part of the Mendip Hills, a range in southwest England consisting of a series of asymmetrical east-west anticlines lying in echelon to give

the WNW-ESE trend (Fig. 5.2). The Mendip Hills are generally flat topped with steep flanks dissected in a few places by narrow gorges as at Cheddar.
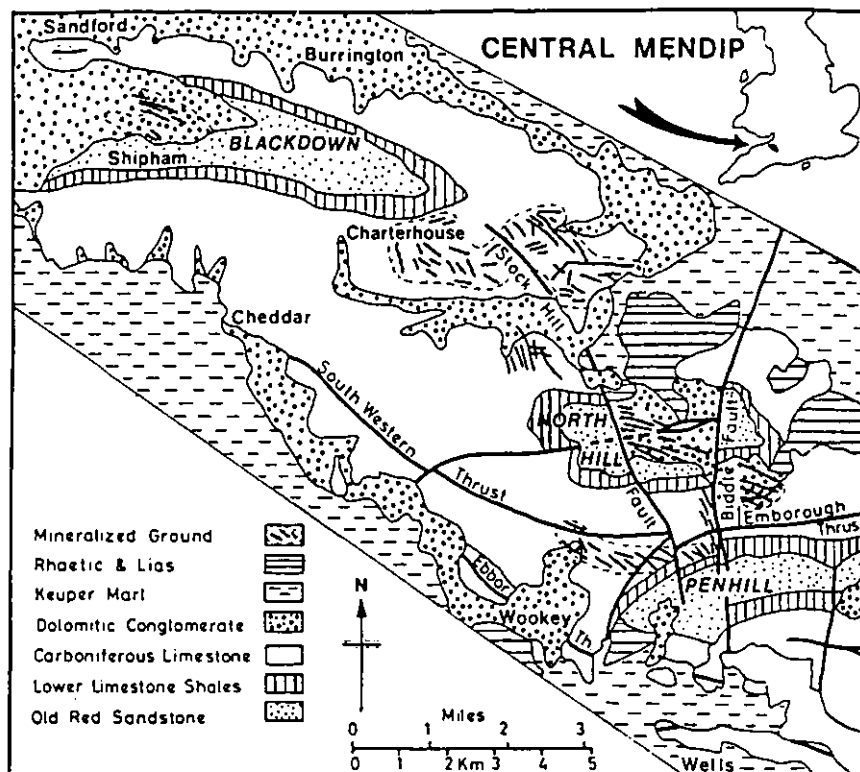
Figure 5.2   Geological map of Central Mendip Hills. From Ford (1976).

The geology of the Mendip Hills has been described in detail by Green and Welch (1965) and Ford (1976) has summarised the geology and discussed the ore genesis. Gough (1967) provides a comprehensive review of the mining activities since pre-Roman times until the late 19th century.

The stratigraphic sequence of the area around Shipham consists of Devonian Old Red Sandstone, Carboniferous Limestone Series, Triassic Dolomitic Conglomerate and Pleistocene Head deposits (Fig. 5.3). The Devonian Old

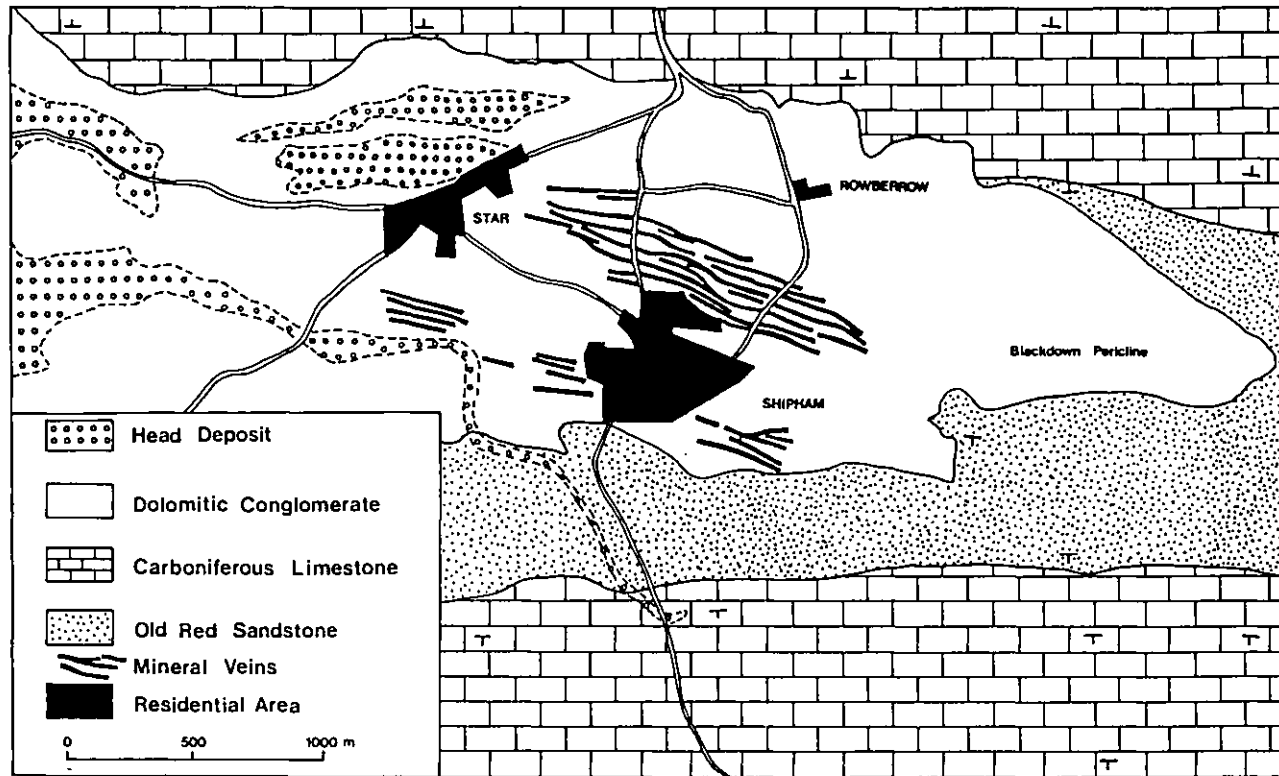Figure 5.3   Geology of the area around Shipham, Central Mendip Hills. From Geological Survey of Great Britain (England and Wales), Sheet ST45.

Legend:
- Head Deposit
- Dolomitic Conglomerate
- Carboniferous Limestone
- Old Red Sandstone
- Mineral Veins
- Residential Area

0   500   1000 m

STAR
ROWBERROW
SHIPHAM
Blackdown Pericline

Red Sandstone includes conglomerates, sandstones and marls that crop out in the core of the Blackdown pericline, making higher ground. The Carboniferous Limestone Series has two divisions, the Lower Limestone Shales and the Carboniferous Limestone which consists of well bedded massive limestones with oolitic calcarenites, calcilutites, chert, dolomites, and thin shales and sandstones towards the top. The Carboniferous Limestone forms the limbs of the Blackdown pericline, the beds commonly dipping at 70° on the north flank while on the south dips of 30° are common. The Dolomitic Conglomerate is largely composed of fragments of Carboniferous Limestone, sometimes dolomitised or haematised, cemented in a matrix of gravel, sandy marl or fine-grained limestone debris, which were originated during the Triassic times by erosion of the Mendips, following the post-Carboniferous folding and uplift. In the immediate vicinity of Shipham, the Dolomitic Conglomerate lies directly on the Old Red Sandstone as the intervening Carboniferous rocks have been eroded. The Head deposits consist mainly of chert and limestone debris derived from the Carboniferous Limestone and Dolomitic Conglomerate, mixed with sand and clay, being the products of solifluction under periglacial conditions during the Pleistocene.

The Pb-Zn mineralisation in the Shipham site, on the core of the Blackdown pericline, is intense and occurs in the Dolomitic Conglomerate as veins trending east-west parallel to the bedding or as fissure fillings. Since the past mining activities have removed and obscured the veins, the pattern of surface expression of the ore deposits has

been reconstructed by examination of surface relics (Green and Welch, 1965). The main ore of lead was galena (PbS) and that of zinc smithsonite (calamine, $Zn\ CO_3$); sphalerite (ZnS) was sometimes present in small amounts. The dominant gangue minerals were calcite ($CaCO_3$) and baryte ($BaSO_4$). According to Ford (1976), the ore genesis can be attributed to hydrothermal fluids that migrated from adjacent basins and mineralised preferentially the Dolomitic Conglomerate or rocks of the Carboniferous Limestone succession that were closest either to the faults or to the Dolomitic Conglomerate, probably during the early Jurassic times with a period of oxidation possibly in the late Tertiary times.

Lead mining has been carried on in Mendip from pre-Roman times, being most active in Roman times and again from the 14th century until the late 19th century. Calamine, the zinc ore, was mined for the first time in the middle 16th century and reached its peak in the 18th century when lead mining was declining and finally stopped in the middle 19th century (Gough, 1967). The calamine mining started in the late 16th century at Shipham, where the ore was extracted largely by hand from a series of shallow bell-pits and then calcined at or near the site of extraction prior to transportation to Bristol for use in the brass industry. Lead ore was also produced at Shipham though in lesser quantities (Goodman, 1979).

The presence of the underlying Pb-Zn mineralisation in the Dolomitic Conglomerate, coupled with the past mining activities that brought ore to the surface, have produced in

the soils around Shipham anomalous levels of Pb, Zn, and Cd which replaces zinc in the crystal lattice of zinc minerals.

5.3   SOILS

The most important groups of soils around Shipham are those derived from Old Red Sandstone (Maesbury Series), Carboniferous Limestone (Lulsgate Series), and Dolomitic Conglomerate (Wrington Series), which have been described in detail by Findlay (1965).

The soils of the Shipham site are mainly freely drained brown earths of the Wrington series. These soils are red brown with rubbly sub-soil and a neutral pH.

Goodman (1979) and Matthews and Thornton (1980) took topsoil (0-15 cm) samples at 50m and 100m intervals along transects running across the main lithologies and soil types and through the mineralised site in order to gain information about the distribution of metals in the soils and to investigate the extent of metal contamination due to the past mining and processing activities. Their results show that the concentration of Cd, Pb, and Zn in the samples of soils derived from the Carboniferous Limestone and Dolomitic Conglomerate are elevated, whereas soils developed on the Old Red Sandstone are not enriched in metals. The majority of the soils sampled on the Dolomitic Conglomerate parent material and covering an area of about 8 sq. km in the vicinity of Shipham contain from 10 to 40 ppm of Cd, 210 to 1000 ppm of Pb, and 1500 to 4000 ppm of Zn. These values

rise steeply over the site of mineralisation lying immediately north of the Shipham Village, to maximum values of 600 ppm of Cd, 1 per cent of Pb, and 6 per cent of Zn. These unusually high amounts of Cd, Pb, and Zn, large enough to inhibit plant growth, are due primarily to the underlying mineralisation and secondarily to the past mining activities that brought ore to the surface. Ore washing and calcining operations in the vicinity of Shipham may have led to further contamination, however this is difficult to assess since the exact position of the processing sites have been lost.

5.4   CLIMATE

The climate of the region around Shipham can be classified in a simplified way, as warm temperate and humid. The meteorological data collected by the Long Ashton Station, which is situated 15 km north of Shipham, and published in the Monthly Weather Report of The Meteorological Office show that the mean rainfall is 879 mm a year and the mean annual temperature is 10°C. The average daily bright sunshine is 4 hours, with 60 per cent of the days having high or total cloud cover at 09.00 hrs. These weather conditions determine that the region is humid and often very cloudy.

In the regional climatic classification of the British Isles proposed by Gregory (1976), the climate of the Shipham region is classified as BMw, where B means a growing season (accumulated temperature above 6°C) of 7 or 8 months,

M means an annual rainfall between 750 and 1250 mm, and w means a rainfall maximum in the winter half of the year.

5.5   VEGETATION

The main vegetation cover types in the vicinity of Shipham consist of grasslands and arable lands. The other types include the coniferous Mendip Forest and the heathland that lie to the east of the village and some patches of deciduous woodlands scattered around the area (see Fig. 5.1).

Of particular interest to this study is the grassland growing over the mineralised site located immediately north of the Shipham Village (see Fig. 5.4). This vegetation cover of grasses and herb species show biogeochemical and geobotanical anomalies that have been induced by the high metal concentrations of the soils which contain up to 600 ppm of Cd, 1 per cent of Pb, and 6 per cent of Zn.

Matthews and Thornton (1979, 1980, 1981), from the Applied Geochemistry Research Group of Imperial College, investigated the biogeochemical anomaly present on the vegetation around Shipham in order to determine the metal uptake by different plant species on soils with varying degrees of metal concentrations and to investigate seasonal variations in plant metal content. The aerial parts (leaves and shoots) of individual species were collected and analysed for Cd, Pb, and Zn at approximately monthly

Figure 5.4   View from the Shipham Village looking
              northwest, showing in the foreground
              the vegetation cover of grasses and
              herb species over the mineralised site.

intervals over the period April 1979 to April 1980 and then
in alternate months until January 1981. The results have
shown that plant metal content broadly reflect those of the
soil and that the metal content increases as the soil metal
levels rise.   However, this does not occur in a linear
fashion and, hence, despite the very high soil metal
concentrations on the mineralised site, plant metal contents
are only moderately high, except for some herb species.
Although the vegetation growing over the mineralised site is
biogeochemically anomalous, low metal "availability" in the
soil for plant uptake or plant metal tolerance mechanisms
(see Section 4.2) might explain the lack of a higher metal
content.   Figure 5.5 shows the Cd content of the main
species on the basis of dry weight.
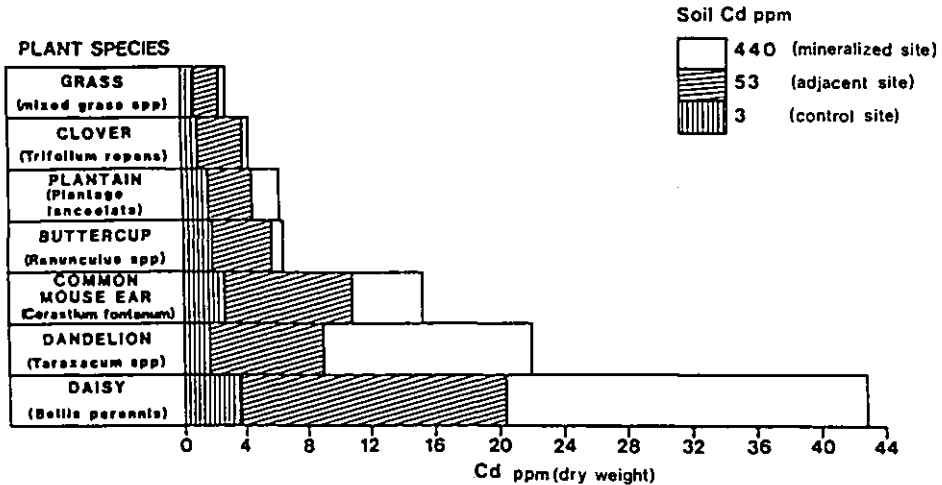
Figure 5.5   Mean Cd content of plants sampled on six occasions between January 1980 and September 1980 at three sites with different soil Cd concentrations. From Matthews and Thornton (1981).

The results have also shown that there are variations in Cd, Pb, and Zn contents of plant species, which are more pronounced for Cd and seem to be dependent on the plant species and related to the specific metal. Grasses were found to have relatively low metal contents when compared with herb species, as illustrated for Cd in Figs. 5.5 and 5.6.

The continuous sampling of vegetation on a monthly basis has revealed that the plants metal content change with season (Fig. 5.7). Maximum values of metal content occur during the winter months, the variation being especially pronounced for Pb though also occurring with Zn and Cd. However, analysis of whole plants have shown that the increased metal content in the aerial parts of the plant corresponds to a decrease in root metal content, thus establishing that the increased metal burden in the aerial
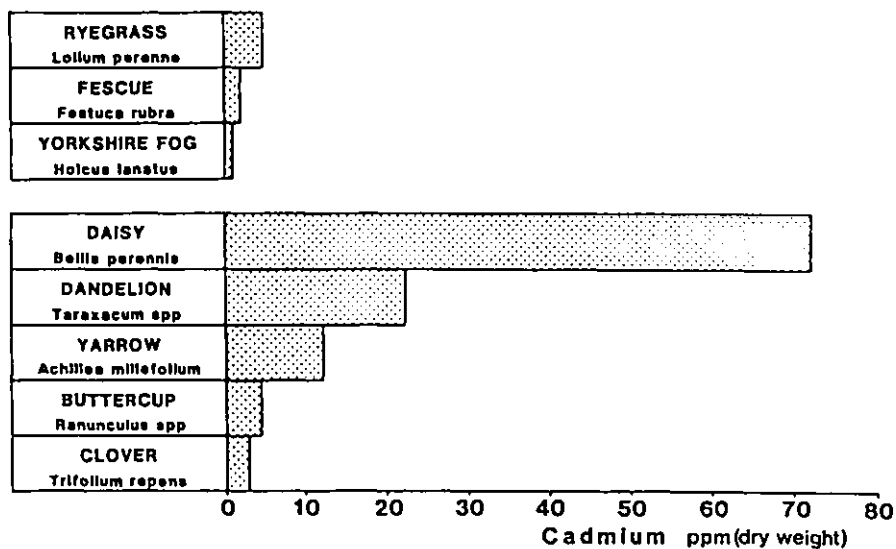
Figure 5.6   Variations in Cd content of plant
              species at Shipham.   From Matthews and
              Thornton (1981).
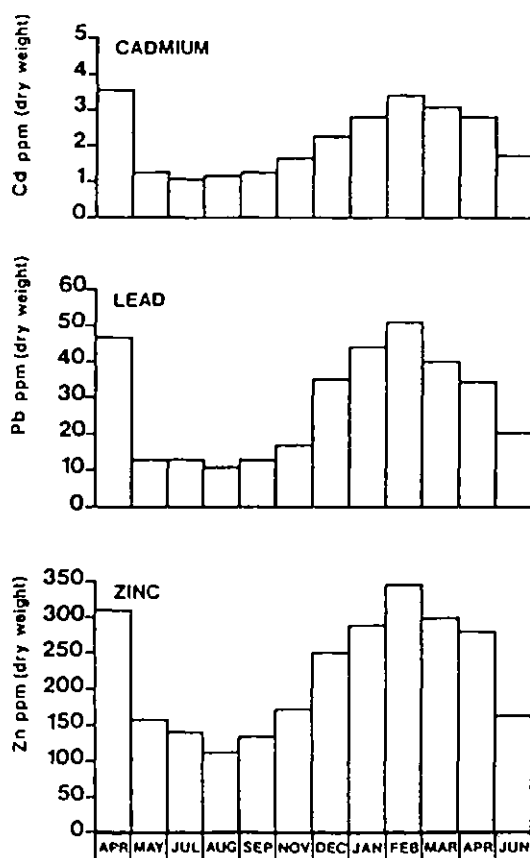
Figure 5.7   Seasonal variation of metal content in
              Holcus lanatus (Yorkshire fog) sampled
              on the mineralised site at Shipham.
              From Matthews and Thornton (1981).

parts of plant species during the winter months is not due to increased uptake but to remobilisation of metals within the plant (Matthews and Thornton, 1981).

In addition to the biogeochemical anomaly described above, the high soil metal content of the mineralised site has also induced geobotanical anomalies on the vegetation canopy. The types of geobotanical anomalies (see section 4.3) shown by the vegetation are the following: the occurrence among the herb species of Thlaspi calaminare, an indicator plant of Zn mineralisations; a reduced vegetation density, including some bare patches; and chlorosis (Fig. 5.8), usually more apparent and widespread in late winter and early spring though during this time of the year the plant metal content is decreasing.

Figure 5.8   Detailed view of the rather patchy vegetation cover of grasses and herb species over the mineralised site, showing apparent signs of chlorosis.

5.6   SELECTION OF LANDSAT IMAGERY

Although the Landsat images the same area every period of 18 days and has been operating for a considerable number of years, very few cloud-free images are available over the Shipham test site since the weather conditions of this area determine that most of the days are overcast (see Section 5.4).

After a search through the archive of images held by the Remote Sensing Unit of the Space Department, Royal Aircraft Establishment (RAE), which is the distribution centre for Landsat products in UK, three images without cloud cover over the Shipham test site were found and selected in order to carry out the present multitemporal Landsat study (Table 5.1).

Path	Row	Acquisition Date	Acquisition Time	Solar Elevation Angle	Solar Azimuth Angle
219	24	27 May 1977	10:09 hrs.	51°	138°
219	24	9 March 1980	10:24 hrs.	29°	145°
219	24	2 October 1980	10:17 hrs.	31°	152°

Table 5.1   Data on the selected Landsat MSS images.

5.7   RESULTS OF THE REMOTE SENSING STUDY

5.7.1   Introduction

As the aim of this thesis was to examine the feasibility of using multitemporal Landsat MSS remote sensing data to detect geobotanical anomalous vegetation –

vegetation which shows visual signs of metal stress - and to determine its spectral response pattern in relation to the surrounding vegetation, and considering that these features are normally subtle and small in size, it was realised from the onset of the research that if the results were going to be successful it would be necessary to fully utilise the new opportunities and benefits offered by digital image processing such as the ability to produce large scale images of good quality and to aid the extraction of information for direct visual interpretation or computer-aided classification. Hence, an I^2S System 500 Digital Image Processing System has been used throughout to process the three Landsat scenes selected for this multitemporal remote sensing study (see Section 5.6).

The first step on the image processing sequence was to sample from the three Landsat scenes, at full resolution, the subscenes depicting the area under study and register them. After this, preprocessing techniques were applied to correct the images, as described in Section 3.2, in order to create a more accurate rendition of the original data in terms of its radiometric and geometric properties for display and further processing. Then, various enhancement techniques were carefully applied to the images with the purpose of aiding their analysis and visual interpretation and providing a suitable input for computer-aided classification.

5.7.2 Visual Analysis and Interpretation

The beginning of the investigation involved the visual analysis of the unenhanced images over Shipham and the generation of their histograms for the four MSS bands (Fig. 5.9), in order to assess the relative and absolute brightness of the features on the image and decide on the necessary enhancements to facilitate the extraction of the information required.

The overall brightness and contrast of these images was found to be low, especially on the winter and autumn images whose histograms on Fig. 5.9 show a smaller range of grey levels than the spring image. Thus, available contrast enhancement techniques were applied to the images. Of the several techniques used, the linear contrast enhancement technique provided the best results from which false colour composites of the three images were obtained.

Visual analysis and interpretation of the contrast enhanced bands of the images and their false colour composites revealed that the Shipham geobotanical anomaly is best seen on the spring image (May 1977), after the peak in plant's metal content, whereas the winter image (March 1980) which is near to the peak and the autumn image (October 1980) show the anomaly very poorly (see Fig. 5.10). The false colour composite and the mosaic with the four bands of the May 1977 image subscene displayed on Figs. 5.11 and 5.12 respectively, show the location of the geobotanical anomaly and illustrate its degree of differentiation from the surrounding vegetation and the other land cover types of the area.
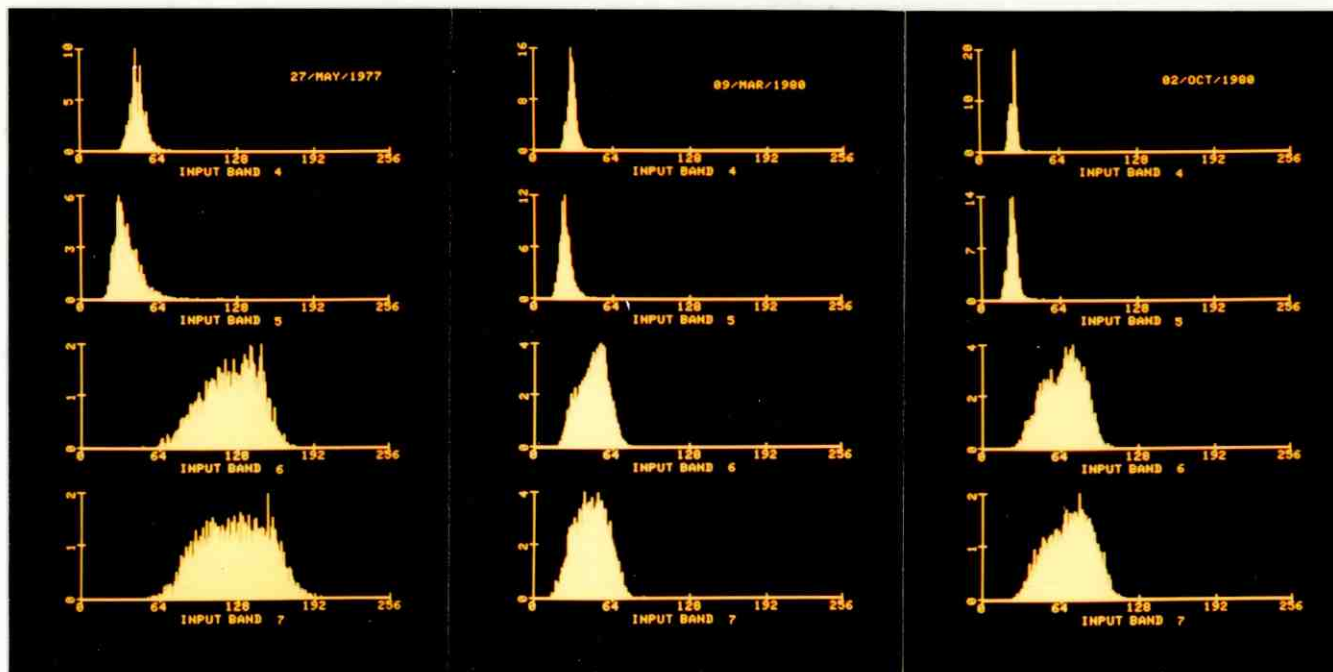
Figure 5.9   Histograms of the unenhanced image subscenes of Shipham.   The
vertical axis indicates the number of pixels and the
horizontal axis the grey levels.

On the four band display (Fig. 5.12) it can be seen that the pixels representing the geobotanical anomaly, outlined in red, show in general a higher reflectance on the visible bands (4 and 5) and a lower reflectance on the near infrared bands (6 and 7) than the background vegetation not affected by the mineralisation, which bounds the anomaly on its west, north and east side whereas its south side is bounded by the Shipham Village. This is in agreement with the general trend observed on the reflectance studies of metal stressed vegetation reviewed and discussed in Section 4.2. The increased reflectance of the geobotanical anomaly on the visible bands could be explained by two character-istics of this feature. One is the presence of chlorosis or yellowing of leaves (see Fig. 5.8) due to decreased chloro-phyll production caused by metal stress. The reduced chlorophyll concentrations results in the plants absorbing less in the chlorophyll absorption bands and hence having a higher reflectance on the visible region of the spectrum, particularly in the red portion (Hoffer, 1978) which is sensed by band 5. The other characteristic is the reduced vegetation density of the geobotanical anomaly; a decrease in the leaf area index and consequently an increase in the amount of soil background seen by the sensor can cause a higher reflectance in the visible and a lower reflectance in the near infrared (Colwell, 1974). Therefore, the reduced vegetation density may also account for the lower reflectance on the near infrared bands.

The false colour enhancement (Fig. 5.11) illustrates more clearly the differentiation in reflectance between the
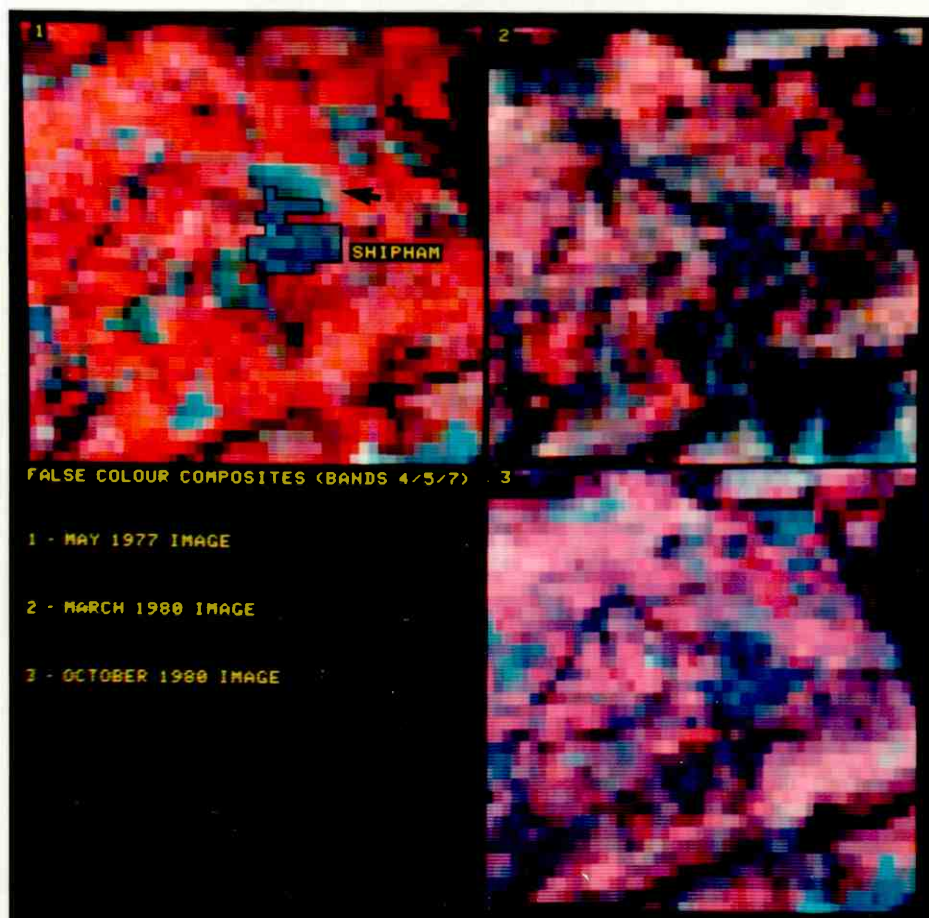
Figure 5.10   Mosaic of the false colour composites
of the area around the Shipham
Village, outlined in black on the
image in the top left quadrant,
showing the seasonal variation on the
detection of the geobotanical anomaly
(arrowed). Image scale is 1:50,000.

FALSE COLOUR COMPOSITE (BANDS 4/5/7) MAY 77 IMAGE

MENDIP FOREST

SHIPHAM
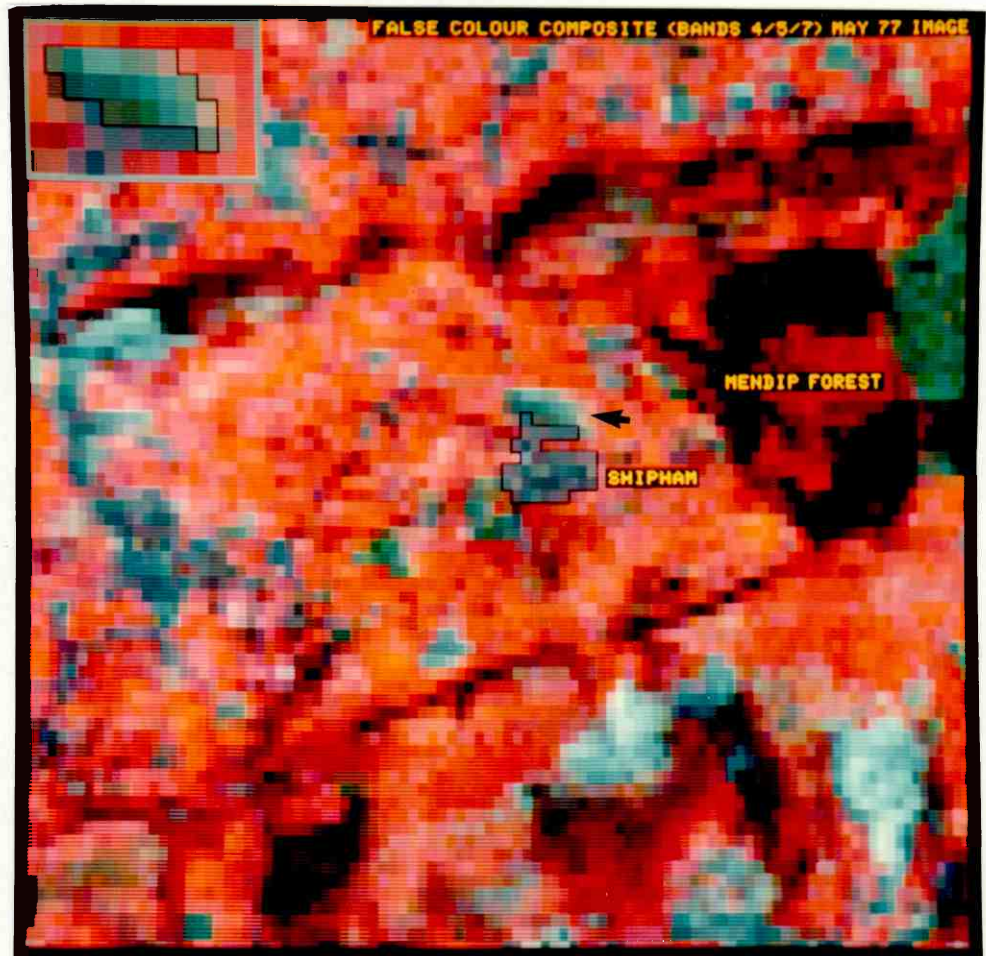
Figure 5.11   Annotated false colour composite of the May 1977 image subscene showing near its centre the geobotanically anomalous vegetation, arrowed, which has a predominantly light blue green colour response and is located immediately north of the Shipham Village, outlined in black. An enlarged view of this feature can be seen on the inset at the top left corner where the pixels representing it have been outlined in black. See text for further explanation. Figure 5.1 illustrates in dashed lines the area covered by this image subscene and shows its main land cover types. Image scale is 1:50,000.
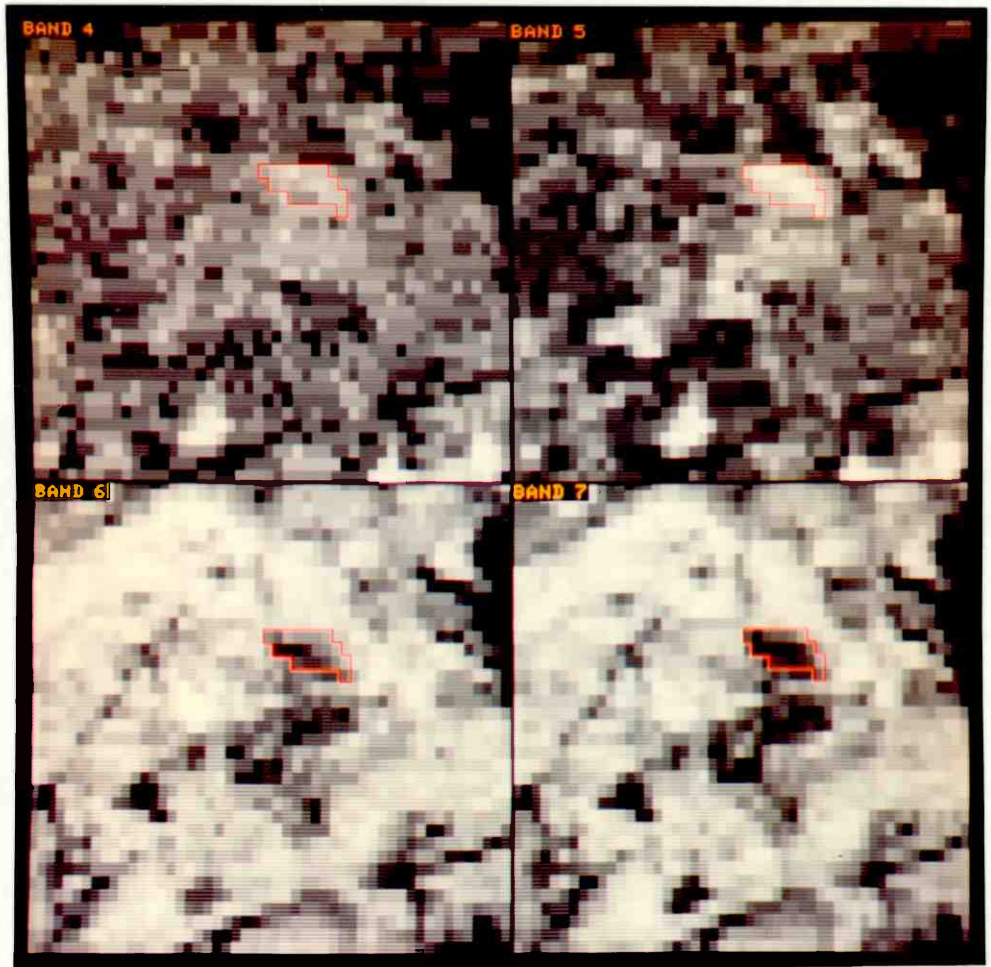
Figure 5.12   Mosaic   showing   the   geobotanical
              anomaly, outlined in red, on the four
              bands of   the   May 1977   image   after
              contract   enhancement.   Note   that   the
              ground   area   represented   on   each
              quadrant   corresponds   to   the   central
              portion   of   Fig.   5.10.   See   text   for
              further   explanation.   Scale   is
              1:50,000.
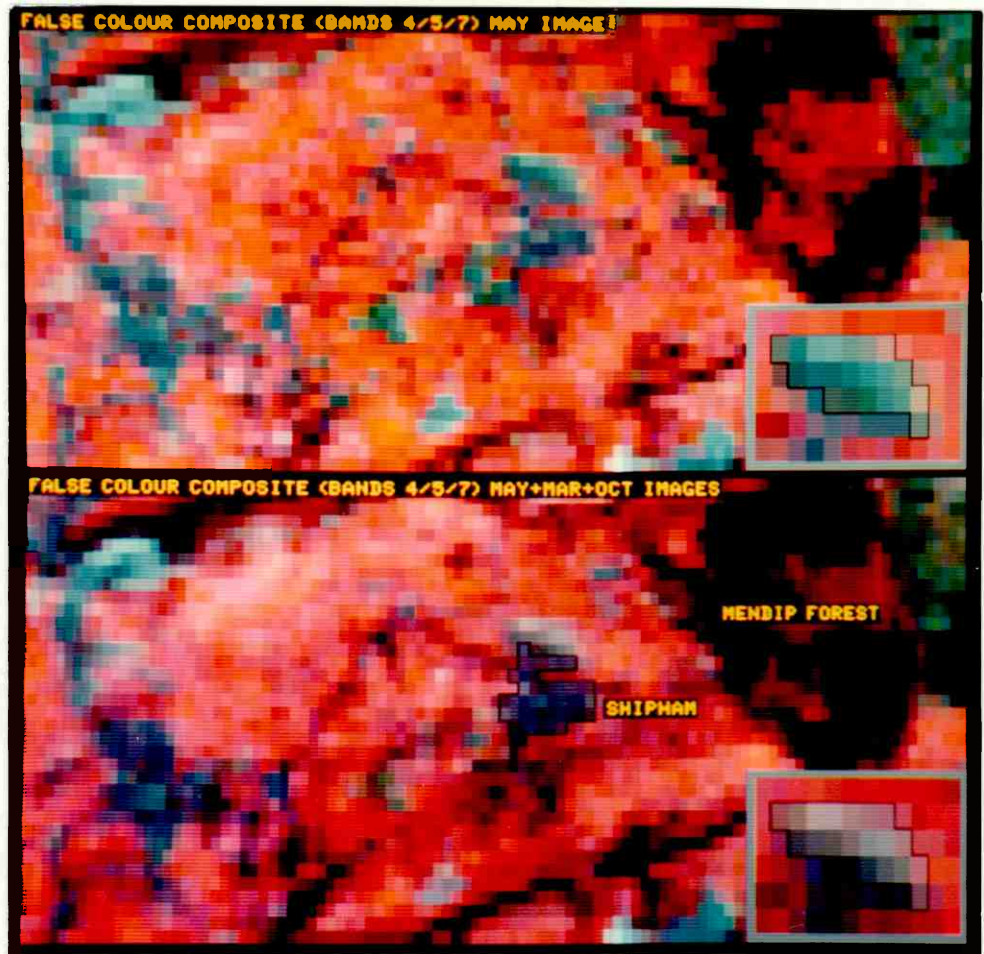
Figure 5.13   Mosaic showing the false colour
composite of the May image, together
with the multitemporal false colour
composite for comparison. Note that on
the multitemporal false colour
composite the geobotanical anomaly
shows a distinct colour response and
can be readily identified. The pixels
representing the geobotanical anomaly
are enlarged and outlined in black on
the insets. Scale is 1:50,000.

geobotanical anomaly, shown in a predominantly light blue green colour, and the background vegetation, shown in a reddish orange to orange pink colour. The variations in colour response for some of the pixels interpreted as representing the geobotanically anomalous vegetation are due to boundary pixels which have spectral contributions from the surroundings.

Additionally, the false colour composite in Fig. 5.11 allows the comparison of the geobotanical anomaly with the other land cover types of the area (see also Fig. 5.1) which show the following colour responses: black and blackish red, varying to dark reddish brown for the coniferous Mendip Forest and the deciduous woodlands; reddish orange to orange pink for arable and grasslands; moderate blue for built-up areas; white to light blue for quarries; moderate green for areas of exposed soil; and a light to moderate blue green for the heathland.

Though the spring image proved to be the most useful to detect and locate the geobotanical anomaly, especially its false colour composite, the visual analysis of its colour responses and their interpretation in terms of land cover types described above show that whereas the geobotanical anomaly can be readily distinguished from the surrounding vegetation and some of the land cover types, its differentiation from others like the heathland is not so obvious. Therefore, in order to investigate the possibility of making the geobotanical anomaly more distinct on the images to facilitate its interpretation, further image

enhancement processing was carried out. Section 3.3 describes the enhancement techniques which were available and have been applied to the images.

The addition of multitemporal images proved to be the most successful technique to discriminate the geobotanical anomaly from some of the other land cover types on the imagery. This enhancement consisted in adding pixel-by-pixel, on an equal weight basis, the contrast enhanced and registered sub-scenes of the three images used in this study. The output image was then used to produce the multitemporal false colour composite shown in the mosaic in Fig. 5.13, together with the May 1977 false colour composite for comparison. Though not uniform, the colour response of the geobotanical anomaly as a whole is distinct and allows it to be readily interpreted.

5.7.3 Computer-Aided Classification

In addition to using enhancement techniques to differentiate more effectively the geobotanical anomaly for visual interpretation, a computer-aided classification of the Shipham subscene was carried out with the objective of assessing the efficiency of this methodology for classifying the geobotanical anomaly.

The method chosen to implement the computer-aided classification was the unsupervised, also called clustering. This method uses only the statistical properties of the image data (pixel values) to identify spectrally distinct

classes in the image data. These spectral classes are subsequently interpreted by relating them to land cover types of interest with the aid of reference data such as maps, ground observations, and other larger scale imagery. In contrast, on the supervised method the land cover types or classes of interest are defined in advance and then their spectral separability is examined through the use of training samples of the image data which represent training sites of known ground conditions. The small size of the geobotanical anomaly, which placed a practical limitation on the use of training samples, was the reason for opting for the unsupervised method. Swain (1978) and Lillesand and Kiefer (1979) give an excellent general description of both approaches, while Townshend and Justice (1980, 1981) discuss the difficulties facing the user when selecting the best approach for image classification and describe in detail the various stages involved in carrying out an unsupervised classification of Landsat MSS data.

The input image selected for classification was the result of the multi-image enhancement (addition of multitemporal images) which provided the best discrimination between the geobotanical anomaly and the other land cover types for visual interpretation. The clustering algorithm applied was the I^2S System 500 application program called "cluster", described in the user's manual (International Imaging System, 1981). The cluster program implements the unsupervised classification at display level by using a variety of hardware features in the Model 70 image processing computer, which has only four eight bit Refresh

Memory channels in the present configuration of the system available for this study. This configuration placed a restriction on the use of all the four bands of the input image chosen for classification since the cluster program utilises two of the four channels to hold the interim and output results from the clustering, leaving only two channels free to hold the input images. This means that only two bands of an image can be used as input at any one time. Hence, bands 5 and 7 were chosen since they provide the best view for the visible and near infrared bands when compared with bands 4 and 6, respectively. The input files had 102 samples by 72 lines, totalling 7344 pixels for each band.

The cluster program allows the initial number of classes to be specified by the user but other parameters can cause classes to be merged or be split during the iterations that take place. The number of classes specified was 16 and Table 5.2 shows that 16 classes plus one reject class were generated. This table also shows the statistics for each spectral class and their interpretation in terms of land cover types which is described below.

The result of the classification was displayed on the TV monitor screen as a black and white classification map where black was assigned to the reject class and different grey tones to each of the 16 classes. Since the human eye has a greater ability to discriminate colours than grey tones, the classification map was pseudocoloured to enhance the difference between the classes. The result of

Spectral Class Number	Number of Pixels	Mean		Standard Deviation		Interpretation of the Spectral Classes
		Band 5	Band 7	Band 5	Band 7	
1	556	13.63	45.70	6.58	13.50	Woodland
2	384	37.74	77.34	6.06	12.57	"
3	431	59.43	75.17	5.74	12.70	Built-up land
4	242	83.09	72.52	9.26	12.83	Heathland
5	471	21.57	91.05	5.75	12.31	Woodland
6	754	37.33	115.16	6.29	9.28	Grassland and arable land
7	523	57.55	115.29	5.66	9.74	"
8	287	80.86	113.40	9.03	10.74	Geobotanical anomaly
9	433	29.13	153.49	4.82	11.18	Grassland and arable land
10	710	43.79	143.16	4.18	8.06	"
11	447	59.84	148.03	4.55	9.42	"
12	188	82.19	148.56	9.25	12.10	"
13	387	35.44	196.42	6.78	11.10	"
14	747	40.53	170.09	4.85	6.82	"
15	416	51.26	181.16	4.30	10.48	"
16	174	69.52	187.76	5.74	14.98	"
Reject	194	155.95	101.66	46.11	37.18	Quarry

Table 5.2   Statistics of the spectral classes generated by the cluster program using bands 5 and 7 as input and their interpretation in terms of land cover types.

the pseudocolour enhancement was then photographed using a fixed-mounted 35mm camera and subsequently enlarged to the scale of 1:50,000. At this scale the outline of the individual pixels could be clearly seen and hence enabled a pixel grid to be drawn from the photography on an overlay, which was then superimposed and closely registered to the area covered by the image on the Ordnance Survey map (sheet 182, Weston-Super-Mare and Bridgwater) having the same scale. Once a satisfactory fit was obtained between the pixel grid and the map, the land cover type of the area covered by each pixel was determined and transferred to the grid, based on the land cover data contained on the Ordnance Survey map and complemented by interpretation of panchromatic aerial photographs on the scale 1:12,000 and ground observations. Then, the pixel grid containing the ground data was overlaid back onto the pseudocoloured classification map and the ensuing comparison between them allowed the interpretation of the spectral classes in terms of land cover types, as listed on Table 5.2. Since there was no evidence to suggest that grassland could be differentiated from arable land, these land cover classes have been merged. The surprising fact which emerged from the interpretation of the spectral classes was that most of the reject spectral class was found to closely match the quarry areas and hence for this reason alone it was considered to be a valid class, though it is not statistically sound. No satisfactory explanation for this can be advanced, mainly because the available I^2S documentation about the cluster program is not particularly detailed. However, it is suspected that the very high

reflectance values of the quarries in band 5 might be responsible for their assignment to the reject class.

Following the interpretation of the spectral classes, the original black and white classification map was used to produce a colour coded classification map (Fig. 5.14), where the spectral classes representing the same land cover type have been merged by assigning them the same colour in order to facilitate the evaluation of the classification accuracy. Then, the pixel grid with the ground information was overlaid to the colour coded classification map and the correctly classified and misclassified pixels were counted. the results are shown in Table 5.3.

Examination of the confusion matrix shows that apart from the high accuracy rate obtained for the grassland and arable land class (86%), which is somewhat responsible for the reasonably good overall classification accuracy (77.6%), the results for the other classes were less satisfactory, specially for the built-up land and heathland classes. Twenty-nine per cent of the heathland was misclassified as built-up land and forty-three per cent of the built-up land was misclassified either as heathland (13%) or grassland and arable land. Also, there was some confusion between the woodland and grassland and arable land since 25% of the woodland was misclassified as grassland and arable land. Though the classification accuracy obtained for the geobotanical anomaly was only 67%, it may be considered good in view of the smallness of this feature and hence its high proportion of boundary pixels. However, the spectral class
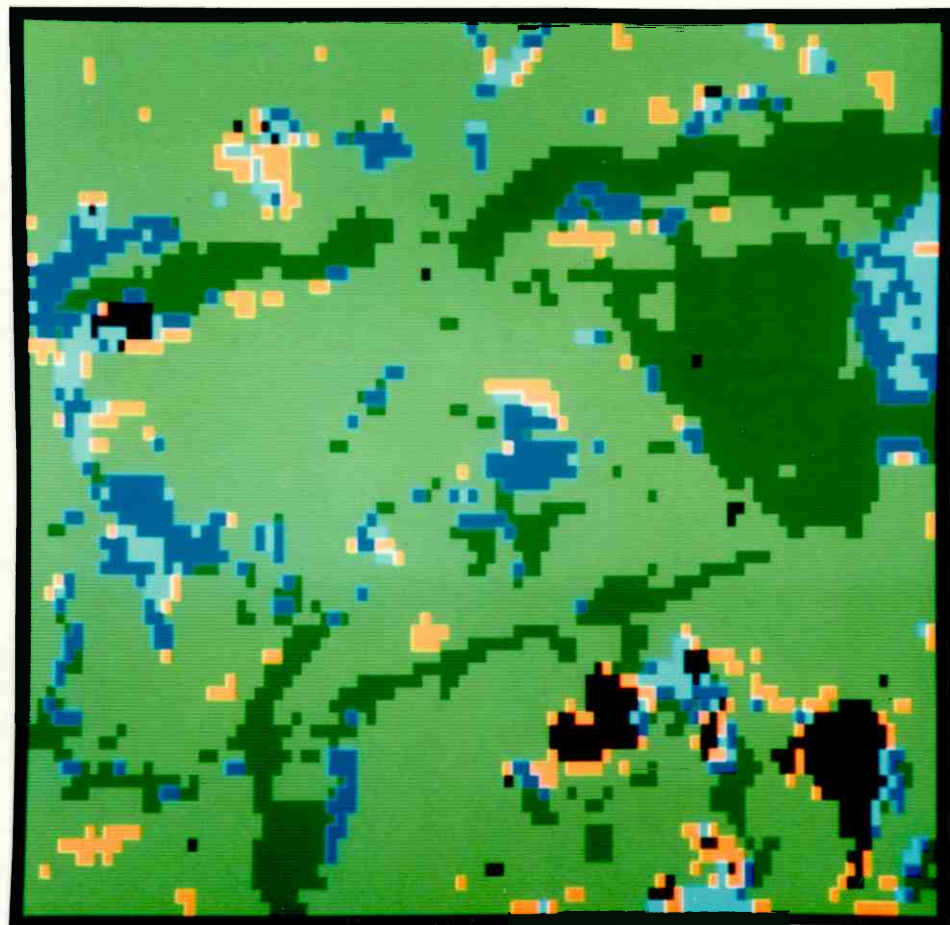
Figure 5.14   Colour coded classification map of the Shipham subscene showing six different classes with the following colours: grassland and arable land in light green; woodland in dark green; built-up land in dark blue; heathland in light blue; geobotanical anomaly in orange; and quarry in black. Scale is 1:50,000.

Actual classes	1 2 5	3	4	6 7 9 10 11 12 13 14 15 16	8	Reject	Total Number of Pixels	Correct Classification (%)
Woodland (1+2+5)	1051	30	9	381	20	9	1500	70
Built-up land (3)	73	255	82	185	18	7	620	41
Heathland (4)	34	60	83	28	5	0	210	40
Grassland and Arable Land (6+7+9+10+11+12+13 +14+15+16)	251	79	54	4153	217	36	4790	87
Geobotanical Anomaly (8)	0	2	5	0	14	0	21	67
Quarry (reject)	2	5	9	32	13	142	203	70
Total number of Pixels	1411	431	242	4779	287	194	7344	

Overall Classification Accuracy = 77.6% (total correct pixels/total pixels)

Table 5.3   Confusion matrix showing the unsupervised classification accuracy results from the Shipham test site.

number 8, which was related to the geobotanical anomaly because it included most of this feature, was found not to be uniquely associated with it. In fact, this spectral class proved to have a strong overlapping contribution from grasssland and arable land that resulted in a decrease of 4.5% in this land cover class accuracy and 3% in the overall accuracy.

An obvious explanation for the overlap of ground information in some of the spectral classes and hence the resulting high degree of misclassification lies probably on the fact that the resources available for implementing the classification prevented the use of all the four bands of the input image. This has almost certainly led to a less subtle spectral discrimination between the land cover types of interest. Moreover, apart from other sources of classification errors such as boundary pixels and the internal variations in spectral response within individual land cover types due, for instance, to their inhomogeneity and to topographic effects such as slope and aspect, some degree of misclassification could be attributable to possible inaccuracies on the ground data contained on the pixel grid used for assessing the classification accuracy. The limitations encountered in precisely matching the pixel grid with the corresponding area on the Ordnance Survey map and also in locating the pixels on the aerial photographs, made the process of determining the ground data of the pixels a complex and difficult one, specially for areas of small and mixed land cover types and of gradual changes.

This increased the chances of producing ground data inaccuracies and, therefore, misclassifications.

5.8   DISCUSSION OF THE RESULTS

The visual analysis and interpretation of digitally enhanced Landsat MSS multitemporal data for the Shipham test site have shown that the vegetation growing over Pb-Zn-Cd mineralised terrain, which constitute both biogeochemical and geobotanical anomalies, could be detected on the spring image (27 May 1977) whereas on the winter (9 March 1980) and autumn (2 October 1980) images it was not apparent.

This variation in detection of the geobotanical anomaly on the multitemporal images seems to be related to seasonal effects because its appearance on the ground also varies according to the time of the year. Though the plant's metal content peaks during the winter months, the visual signs of metal stress such as chlorosis are more apparent and widespread during late winter and spring. Thus, these times of the year are potentially the most suitable for detecting this anomaly. However, the factor that appears to have aided its detection on the spring image is the combination of more intense visual signs of plant metal stress with the progressing spring leaf flush, which have probably enhanced reflectance differences between the anomalous and background vegetation. This suggests that what has been detected on the spring image was a seasonally pronounced difference in chlorophyll stage and vegetation density. The pattern of increased visible reflectance and

decreased infrared reflectance of the geobotanical anomaly, in relation to the background vegetation, is consistent with this assumption. Despite being another possibility, water stress seems unlikely to have aided the detection of this feature because this area has an annual average rainfall of around 900 mm and on the month preceding the acquisition of the spring image received a total rainfall of 45 mm, which is 83% of the average total rainfall for this time of the year (data from Long Ashton Station, published in the Monthly Weather Report of the Meteorological Office).

Therefore, the clear detection of the geobotanical anomaly on the spring image seems more likely to be associated with a seasonally pronounced difference in chlorophyll state and vegetation density between this anomaly and the background vegetation due to a combination of plant metal stress and vegetation phenological stage. Indeed, the importance of vegetation phenology in aiding the detection of biogeochemical and geobotanical anomalies have also been noted on the Landsat studies carried out by Levine (1975), Lefevre (1980), and Darch (1982). Another factor that might have further aided the clear detection of this feature on the spring image was image quality because this image showed better quality than the other two images, an indication of which is given by its greater range of grey levels that is shown by the histograms of the unenhanced data in Fig. 5.7.

Even though the spring image was the most useful for detecting the Shipham geobotanical anomaly, its best

discrimination was achieved by the false colour composite of the multi-image enhancement - addition of the contrast enhanced multitemporal images - shown in Fig. 5.13. These results suggest that the analysis and integration of the seasonal variations in spectral reflectance from the geobotanical anomaly can provide a valuable basis for both its detection and interpretation and, additionally, underline the value of multitemporal remote sensing data sets. However, the full utilisation of the multitemporal characteristic of the Landsat data to investigate the persistence of the seasonal effects was hindered by the fact that cloud free and high quality images for the Shipham area were rare, despite the fact that the Landsat satellites have been orbiting since July 1972.

The spatial resolution of the Landsat MSS data has been regarded as a considerable limitation to the study of features as small as the Shipham geobotanical anomaly. Nevertheless, the results of this study show that this may be lessened by fully utilising the benefits of digital image processing techniques. The application of these techniques, which were facilitated by the digital character of the data transmitted from the Landsat satellites, allowed efficient registration of the multitemporal data sets and generation of full resolution, large scale images of improved quality for display and enhancement that substantially aided the extraction of the full information content of the Landsat multitemporal images by both visual interpretation and computer-aided classification.

The most efficient enhancement techniques for visually detecting and identifying the Shipham geobotanical anomaly on the images were contrast stretching, additive colour composition, and mainly addition of multitemporal images. The products of other enhancement techniques applied to the images proved to be much less useful and, in some cases, disappointing though some of them were considered most useful in other remote sensing studies reported in the literature. For instance, ratioing was used successfully to detect geobotanical anomalies (Lyon, 1975; Bolviken, 1977), hydrothermally altered rocks (Rowan et al., 1975), and gossans overlying sulphide deposits (Blodget, 1978). This inconsistency tends to underline the views that the success of a particular technique is dependent on both the scene (Goetz et al., 1975) and on the nature of the information required by the interpreter (Gillespie et al., 1980), thus preventing generalisations concerning the applicability of the enhancement techniques.

The classification accuracy of 67% obtained for the geobotanical anomaly, using an unsupervised computer-aided classification method, may be regarded as an encouraging result if we consider that the errors of omission (33%) may be largely attributable to boundary pixels that constitute a high proportion of this feature due to its smallness. However, if we consider the results from the point of view of errors of commission (95%) they are far from satisfactory since 273 out of the total of 287 pixels classified as geobotanical anomaly (see Table 5.3 and Fig. 5.14) are not

believed to represent geobotanical anomalies. Nevertheless, these pixels might suggest potential targets for a more detailed field study for mineral exploration and hence be of value in reducing the area to be prospected. In addition to the fact that the available resources to implement the classification limited the number of bands of an image that could be utilised to only two and thus may have had a negative effect on the results, as mentioned above, the classification performance could also have been influenced by the multitemporal nature of the input selected for classification. This might have introduced other variables into the classification process but their effects are difficult to evaluate, however.

CHAPTER SIX

CONCLUSIONS

The results of this investigation seem to provide further evidence that the discrimination of metal-stressed vegetation from unstressed vegetation by remote sensing data is possible, even using the low spectral and spatial resolution images of the Landsat MSS sensor. However, the Landsat multitemporal remote sensing study of the Shipham test site appears to indicate that the success in detecting and interpreting geobotanical anomalies may be strongly influenced by seasonal effects.

As suggested in the discussion of the results, the interaction of seasonal variations in the intensity of visual signs of plant metal stress with vegetation phenology might have been the factor which increased differences in chlorophyll state and vegetation density and, hence, differences in reflectance between the geobotanical anomaly and the background vegetation to a level that allowed the clear detection of the geobotanical anomaly on the spring image, whereas on the winter and autumn images it seems not to have given rise to sufficient reflectance contrasts. However, the integration of these seasonal variations in spectral reflectance, through the addition of multitemporal images, allowed the clear identification of the Shipham geobotanical anomaly by visual interpretation. This enhancement technique

may prove to be a valuable tool for the interpretation of similar seasonally pronounced geobotanical anomalies. Though the application of an unsupervised computer-aided classification to the image obtained by this multi-temporal enhancement technique has correctly classified most of the geobotanical anomaly, the classification can be considered only partially successful due to the considerable errors of commission caused by pixels which are not believed to be geobotanical anomalies but have been classified as so.

Therefore, the utilisation of images acquired at several times of the year, with emphasis on the periods of phenological changes, coupled with a proper understanding of the seasonal pattern of plant metal stress of the area seems to offer the best possibilities for both detection and interpretation of geobotanical anomalies. However, the efficient implementation of the multitemporal approach may be prevented in certain areas because of the scarcity of cloud-free and good quality Landsat images. Thus, apart from the advantages of finer spectral and spatial resolution in remote sensing data, the study of geobotanical anomalies would also benefit from an improved temporal resolution because it would increase the chances of availability of suitable multitemporal imagery. Though the Landsat 4, launched on 16 July 1982, has a temporal resolution (16 days) that is only slightly better than that of the other Landsat satellites (18 days), its Thematic Mapper (TM) sensor has considerable improvements over the MSS sensor. These are: increased number of bands, generally of narrower bandwidths, designed primarily for sensing vegetation-

related information; a greatly improved spatial resolution (30m) over that of the MSS (79m); and a much better radiometric sensitivity than the MSS. In addition, the grey level digital output for all bands have been increased from 64 to 256 levels (NASA, 1982). These characteristics of the TM data are likely to allow a better discrimination of geobotanical anomalies as small as the one at Shipham, which will not only facilitate their visual interpretation but also will increase their computer-aided classification accuracy by reducing their high proportion of boundary pixels. Moreover, it may increase the chances of detecting areas of more subtle metal stress, not enough to produce apparent signs of plant metal stress on the vegetation such as, for instance, chlorosis and changes in vegetation density which are more amenable to detection by remote sensing.

In conclusion, though the results of this study suggest that it is possible to detect geobotanical anomalies using digitally processed, presently available Landsat MSS remote sensing data, the new developments in sensor technology brought into the TM sensor and advanced for future satellites are likely to increase considerably the efficiency of remote sensing techniques for their detection. However, the geobotanical remote sensing approach to mineral exploration is not expected to become a definitive solution to the problem of locating hidden mineral deposits, but rather another useful technique that should be used in conjunction with other exploration techniques to aid the search for new mineral resources.

REFERENCES

ALDRICH, D.G. and TURREL, F.M. (1951). Effect of Acidification on Some Chemical Properties of a Soil and the Plants Grown Thereon. Soil Science 70, 457-471.

ANTONOVICS, J., BRADSHAW, A.D. and TURNER, R.G. (1971). Heavy Metal Tolerance in Plants. Advances in Ecological Research 7, 1-85.

BIRNIE, R.W. and DYKSTRA, J.D. (1978). Application of Remote Sensing to Reconnaissance Geologic Mapping and Mineral Exploration. In: Proceedings of the 12th International Symposium on Remote Sensing of Environment, Vol. 2, pp.795-804.

BLODGET, H.W., GUNTHER, F.J. and PODWYSOCKI, M.H. (1978). Discrimination of Rock Classes and Alteration Products in Southwestern Saudi Arabia with Computer-Enhanced Landsat Data. NASA Technical Paper 1327, Goddard Space Flight Center, Greenbelt, Maryland, 34pp.

BOLVIKEN, B., HONEY, F., LEVINE, S.R., LYON, R.J.P. and PRELAT, A. (1977). Detection of Naturally Heavy Metal Poisoned Areas by LANDSAT-1 Digital Data. Journal of Geochemical Exploration 8, 457-471.

BROOKS, R.R. (1972). Geobotany and Biogeochemistry in Mineral Exploration. Harper and Row, New York, 290pp.

BROOKS, R.R. (1973). Biogeochemical Parameters and their Significance for Mineral Exploration. Journal of Applied Ecology 10, 825-836.

BROOKS, R.R. (1979). Indicator Plants for Mineral Prospecting - A Critique. Journal of Geochemical Exploration 12, 67-78.

CANNEY, F.C. (1975). Development and Application of Remote Sensing Techniques in the Search for Deposits of Copper and Other Metals in Heavily Vegetated Areas. Status Report, June 1975, U.S. Geological Survey, Reston, Virginia, 42pp.

CANNEY, F.C., WENDEROTH, S. and YOST, E. (1971) Relationship Between Vegetation Reflectance Spectra and Soil Geochemistry: New Data from Catheart Mountain, Maine. In: Third Annual Earth Resources Program Review, Houston, Texas, NASA Johnson Space Flight Center, Vol. 1, pp. 18-1 to 18-9.

CANNON, H.L. (1957). Description of Indicator Plans and Methods of Botanical Prospecting for Uranium Deposits on the Colorado Plateau. U.S. Geological Survey Bulletin 1030-M, pp. 399-516.

CANNON, H.L. (1960a). Botanical Prospecting for Ore Deposits. Science 132 (3427), 591-598.

CANNON, H.L. (1960b). The Development of Botanical Methods of Prospecting for Uranium on the Colorado Plateau. U.S. Geological Survey Bulletin 1085-A, 50pp.

CANNON, H.L. (1979). Advances in Botanical Methods of Prospecting for Minerals. Part I - Advances in Geobotanical Methods. In: Geophysics and Geochemistry in the Search for Metallic Ores, Peter J. Hood (editor), Geological Survey of Canada, Economic Geology Report 31, pp. 385-395.

CARRARO, C.C. (1973). Reconhecimento de Rocha Mineralisada de Vazantes nas Transparencias Falsa Cor. Report INPE-282-RI/71, Instituto de Pesquisas Espaciais, Sao Jose dos Campos, 28pp.

CHANG, S.H. and COLLINS, W. (1980). Toxic Effects of Heavy Metals on Plants. In: Abstracts of the 6th Annual

William T. Pecora Symposium on Remote Sensing, Sioux Falls, South Dakota, pp. 122-124.

CHAVEZ, P. (1975). Atmospheric, Solar, and M.T.F. Corrections for ERTS Digital Imagery. American Society of Photogrammetry Proceedings, pp. 69-69a.

COLE, M.M. (1977). Landsat and Airborne Multispectral and Thermal Imagery Used for Geological Mapping and Identification of Ore Horizons in Lady Anne - Lady Loretta and Dugald River Areas, Queensland, Australia. Transactions of the Institution of Mining and Metallurgy 86, Section B, 195-215.

COLE, M.M. (1980). Geobotanical Expression of Ore Bodies. Transactions of the Institution of Mining and Metallurgy 89, Section B, 73-91.

COLE, M.M. and LE ROEX, H.D. (1978). The Role of Geobotany, Biogeochemistry and Geochemistry in Mineral Exploration in South West Africa and Botswana - A Case History. Transactions of the Geological Society of South Africa 81, 277-317.

COLE, M.M., OWEN-JONES, E.S. and CUSTANCE, N.D.E. (1974a). Remote Sensing in Mineral Exploration. In: Environmental Remote Sensing - Applications and Achievements, Eric C. Barrett and Leonard F. Curtis (editors), Edward Arnold, London, pp. 50-66.

COLE, M.M., OWEN-JONES, E.S., BEAUMONT, T.E. and CUSTANCE, N.D.E. (1974b). Recognition and Interpretation of Spectral Signatures of Vegetation from Aircraft and Satellite Imagery in Western Australia. In: Proceedings Symposium European Earth Resources Satellite Experiments, Frascati, Italy, European Space Research Organization, pp. 243-287.

COLLINS, W. and CHIU, H.Y. (1979). Signature Evaluation of Natural Targets Using High Spectral Resolution Techniques. In: Proceeding of the 13th International Symposium on Remote Sensing of Environment, Ann Arbor, University of Michigan, Vol. 1, pp. 567-582.

COLWELL, J.E. (1974). Vegetation Canopy Reflectance. Remote Sensing of Environment 3, 175-183.

DARCH, J.P. (1982). A Remote Sensing and Geochemical Study in Mineralized Vegetated Terrain. Ph.D. Thesis, University of London, 289 pp.

EROS DATA CENTER (1981). Landsat 3 Return Beam Vidicon Response Antifacts: A Report on RBV Photographic Product Characteristics and Quality Coding System. EROS Data Center, Sioux Falls, South Dakota, 13 pp.

FINDLAY, D.C. (1965). The Soils of Mendip District of Somerset. Memoir of the Soil Survey of Great Britain, England and Wales (Sheets 279 and 280), Harpenden.

FORD, T.D. (1976). The Ores of the South Pennines and Mendip Hills, England - A Comparative Study. In: Handbook of Strata-Bound and Stratiform Ore Deposits, Elsevier Scientific Publishing Co., Vol. 5 (Regional Studies), pp. 161-195.

GATES, D.M. (1970). Physical and Physiological Properties of Plants. In: Remote Sensing with Special Reference to Agriculture and Forestry, National Academy of Sciences, Washington D.C., pp. 224-252.

GATES, D.M., KEEGAN, H.J., SCHLETER, J.C. and WEIDNER, V.R. (1965). Spectral Properties of Plants. Applied Optics 4(1), 11-20.

GAUSMAN, H.W. (1974). Leaf Reflectance of Near-Infrared. Photogrammetric Engineering and Remote Sensing 40(2), 183-191.

GILLESPIE, A.R. (1980). Digital Techniques of Image Enhancement. In: Remote Sensing in Geology, Barry S. Siegal and Allan R. Gillespie (Editors), John Wiley and Sons, New York, pp.139-226.

GOETZ, A.F.H. and BILLINGSLEY, F.C. (1974). Digital Image Enhancement Techniques Used in Some ERTS Application Problems. Contributions to Geology 12(2), 7-21.

GOETZ, A.F.H., BILLINGSLEY, F.C., GILLESPIE, A.R., ABRAMS, M.J., SQUIRES, R.L., SHOEMAKER, E.M., LUCCHITA, I. and ELSTON, D.P. (1975). Application of ERTS Images and Image Processing to Regional Geologic Problems and Geologic Mapping in Northern Arizona. Jet Propulsion Laboratory Technical Report 32-1597, Pasadena, California, 188 pp.

GOODMAN, J.G. (1979). The Dispersion of Cadmium, Lead and Zinc in Agricultural Soils in the Vicinity of Old Zinc Mines at Shipham, Somerset. M.Sc. Thesis, University of London, 98pp.

GORDON, F. (1980). The Time-Space Relationships of the Data Points (Pixels) of the Thematic Mapper and Multi-spectral Scanner or "The Myth of Simultaneity". NASA Technical Paper 1715, Goddard Space Flight Center, Greenhelt, Maryland, 25 pp.

GOUGH, J.W. (1967). The Mines of the Mendip. David and Charles, Newton Abbot, 270 pp.

GREEN, G.W. and WELCH, F.B.A. (1965). Geology of the Country Around Wells and Cheddar. Memoirs of the Geological Survey of Great Britain 280, HMSO, London, 225 pp.

GREGORY, S. (1976). Regional Climates. In: The Climate of the British Isles, T.J. Chandler and S. Gregory (editors), Longman, pp. 330-342.

HOFFER, R.M. (1978). Biological and Physical Considerations in Applying Computer-Aided Analysis Techniques to Remote Sensor Data. In: Remote Sensing – The Quantitative Approach, P. H. Swain and S. M. Davis (editors), McGraw Hill International, pp. 227-289.

HOFFER, R.M. and JOHANNSEN, C.J. (1969). Ecological Potential in Spectral Signature Analysis. In: Remote Sensing in Ecology, P. L. Johnson (editor), University of Georgia Press, pp. 1-16.

HORIZON (1959). A Flower that Led to a Copper Discovery, Ndola, Zambia. RST Group, V.1., pp. 35-39.

HORLER, D.N.H., BARBER, J. and BARRINGER, A.R. (1980). Effects of Heavy Metals on the Absorbance and Reflectance Spectra of Plants. International Journal of Remote Sensing 1(2), 121-136.

HOWARD, J.A., WATSON, R.D. and HESSIN, T.D. (1971). Spectral Reflectance Properties of Pinus Ponderosa in Relation to Copper Content of the Soil, Malachite Mine, Jefferson County, Colorado. In: Proceedings of the 7th International Symposium on Remote Sensing of Environment, Ann Arbor, University of Michigan, Vol. 1, pp. 285-297.

INTERNATIONAL IMAGING SYSTEM (1981). User's Manual System 500 Digital Image Processing System (Version 2.3). Milpitas, California, 192pp.

KNIPLING, E.B. (1969). Leaf Reflectance and Image Formation on Colour Infrared Film. In: Remote Sensing in Ecology, P. L. Johnson (editor), University of Georgia Press, pp. 17-29.

KNIPLING, E.B. (1970). Physical and Physiological Basis for the Reflectance of Visible and Near-Infrared Radiation from Vegetation. Remote Sensing of Environment 1, 155-159.

KOVALEVSKY, A.L. (1978). Biogeochemical Halos of Ore Deposits. International Geology Review 20(5), 548-562.

LEAVITT, S.W. and GODDELL, H.G. (1979). Evaluation of Bio-geochemical Prospecting Methods in the Search for Sulfide Deposits in the Appalachian Piedmont, Virginia, USA. Journal of Geochemical Exploration 11, 89-100.

LEVINE, S. (1975). Correlation of ERTS Spectra With Rock/ Soil Types in Californian Grassland Areas. In: Proceedings of the 10th International Symposium on Remote Sensing of Environment, Ann Arbor, Michigan, Vol. 2, pp. 975-984.

LILLESAND, T.M. and KIEFER, R.W. (1979). Remote Sensing and Image Interpretation. John Wiley and Sons, New York, 612 pp.

LOVERING, T.S. (1959). Significance of Accumulator Plants in Rock Weathering. Bulletin of the Geological Society of America 70, 781-800.

LYON, G.L., BROOKS, R.R., PETERSON, P.J. and BUTLER, G.W. (1968). Trace Elements in a New Zealand Serpentine Flora. Plant and Soil 29, 225-240.

LYON, R.J.P. (1975a). Correlation Between Ground Metal Analysis, Vegetation Reflectance and ERTS Brightness over a Molibdenum Skarn Deposit, Pine Nut Mountains, Western Nevada. In: Proceedings of the 10th International Symposium on Remote Sensing of

Environment, Ann Arbor, Michigan, Vol. 2, pp. 1031-1044.

LYON, R.J.P. (1975b). Mineral Exploration Applications of Digitally Processed Landsat Imagery. In: Proceedings of the First Annual William T. Pecora Memorial Symposium, Sioux Falls, South Dakota, U.S. Geological Survey Professional Paper 1015, pp. 271-292.

MALYUGA, D.P. (1964). Biogeochemical Methods of Prospecting. Consultants Bureau, New York, 205 pp.

MATTHEWS, H. and THORNTON, I. (1980). Agricultural Implications of Zn and Cd Contaminated Land at Shipham, Somerset. In: Proceedings of the 13th Conference on Trace Substances in Environmental Health, University of Missouri, Columbia, Missouri.

MATTHEWS, H. and THORNTON, I. (1981). Cadmium in the Farming Environment in Shipham. In: Proceedings of the 3rd International Cadmium Conference, Miami, Florida, pp. 106-111.

MATTHEWS, H. and THORNTON, I. (1982). Seasonal and Species Variation in the Content of Cadmium and Associated Metals in Pasture Plants at Shipham. Plant and Soil 66, 181-193.

MOIK, J.G. (1980). Digital Processing of Remotely Sensed Data. NASA SP-431, Goddard Space Flight Center, Greenbelt, Maryland, 330 pp.

MORTVEDT, J.J., GIORDANO, P.M. and LINDSAY, W.L. (editors) (1972). Micronutrients in Agriculture. Soil Science Society of America, Madison, Wisconsin, 666 pp.

MYERS, V.I. (1970). Soil, Water, and Plant Relations. In: Remote Sensing with Special Reference to Agriculture

and Forestry. National Academy of Sciences, Washington D.C., 424 pp.

MYERS, V.I. and ALLEN, W.A. (1968). Electrooptical Remote Sensing Methods as Nondestructive Testing and Measuring Techniques in Agriculture. Applied Optics 7(9), 1819-1838.

NASA (1968). Application of Biogeochemistry to Mineral Exploration. NASA SP-5056, 134 pp.

NASA (1973). Proceedings of the Symposium on Significant Results Obtained from the Earth Resources Technology Satellite-1, NASA SP-327, Washington D.C., Vol. 1, 1730 pp.

NASA (1974). Proceedings of the Third Earth Resources Technology Satellite-1 Symposium. NASA SP-351, Washington D.C., Vol. 1, 1994 pp.

NASA (1982). Landsat Data Users Notes 23. NASA, U.S. Geological Survey, EROS Data Center, Sioux Falls, South Dakota, 16 pp.

NESVETAYLOVA, N.G. (1961). Geobotanical Investigations in Prospecting for Ore Deposits. International Geology Review 3(7), 609-618.

PRESS, N.P. (1974a). Remote Sensing to Detect the Toxic Effects of Metals on Vegetation for Mineral Exploration. In: Proceedings of the 9th International Symposium on Remote Sensing of Environment, Ann Arbor, Michigan, Vol. 3, pp. 2027-2038.

PRESS, N.P. (1974b). Detecting the Toxic Effects of Metals on Vegetation from Earth Observation Satellites. Journal of the British Interplanetary Society 27, 373-384.

RAE (undated). User Guide, 3rd issue. Remote Sensing Unit, Royal Aircraft Establishment, Farnborough, Hants, 75pp.

REEVES, R.G. (editor) (1975). Manual of Remote Sensing. American Society of Photogrammetry, Falls Church, Virginia, 2 Vols.

ROBINSON, W.O., LAKIN, H.W. and REICHEN, L.E. (1947). The Zinc Content of Plants on the Friedensville Zinc Slime Ponds in Relation to Biogeochemical Prospecting. Economic Geology 42, 572-582.

ROSE, A.W., HAWKES, H.E. and WEBB, J.S. (1979). Geochemistry in Mineral Exploration, Second Edition. Academic Press, London, 657pp.

ROSHOLT, B. (1977). Case History of Copper Mineralization With Naturally Copper Poisoned Areas at Raitevarre, Karasjok, Finnmark County, Norway. In: Prospecting in Areas of Glaciated Terrain, Institution of Mining and Metallurgy, pp. 138-139.

ROWAN, L.C., WETLAUFER, P.H., GOETZ, A.F.H., BILLINGSLEY, F.C. and STEWART, J.H. (1974). Discrimination of Rock Types and Detection of Hydrothermally Altered Areas in Southcentral Nevada by the Use of Computer-Enhanced ERTS Images. U.S. Geological Survey Professional Paper 883, 35pp.

SABINS, F.F. (1978). Remote Sensing Principles and Interpretation. W. H. Freeman, San Francisco, 426 pp.

SHORT, N.M., LOWMAN, P.D., FREDEN, S.C. and FINCH, W.A. (1976). Mission to Earth: Landsat Views the World. NASA SP-360, Washington D.C., 459 pp.

SLATER, P.N. (1979). A Re-Examination of the Landsat MSS. Photogrammetric Engineering and Remote Sensing 45(11), 1479-1485.

SLATER, P.N. (1980). Remote Sensing, Optics and Optical Systems. Addison-Wesley Publishing Company, Reading, Massachusetts, 575 pp.

SMITH, R.F. (1978). Geographical Factors Influencing the Distribution of Heavy Metal Tolerant Indicator Species in Parts of the United Kingdom and Europe. Ph.D. Thesis, University of London, 331 pp.

STEINER, D. and SALERNO, A.E. (1975). Remote Sensor Data Systems, Processing and Management. In: Manual of Remote Sensing, Robert G. Reeves (editor), American Society of Photogrammetry, Falls Church, Virginia, Vol. 1, pp. 611-803.

SUITS, G.H. and SAFIR, G.R. (1972). Verification of a Reflectance Model for Mature Corn With Applications to Corn Blight Detection. Remote Sensing of Environment 2(3), 183-192.

SWAIN, P.H. (1978). Fundamentals of Pattern Recognition in Remote Sensing. In: Remote Sensing: The Quantitative Approach, P.H. Swain and S.M. Davis (editors), McGraw Hill Int., pp.136-187.

TALVITIE, J. (1979). Remote Sensing and Geobotanical Prospecting in Finland. Bulletin of the Geological Society of Finland 51, 63-73.

TARANIK, J.V. (1977). Reference Materials on the Character- istics of the Landsat System for Mineral and Petrol- eum Exploration. Unpublished reference materials available from Applications Branch, EROS Center, U.S. Geological Survey, Sioux Falls, South Dakota, 52 pp.

THOMAS, J.R., MYERS, V.I., HEILMAN, M.D. and WIEGAND, C.L. (1966). Factors Affecting Light Reflectance of

Cotton. In: Proceedings of the 4th International Symposium on Remote Sensing of Environment, Ann Arbor, Michigan, pp. 305-312.

TOWNSHEND, J.R.G. (1981a). The Spatial Resolving Power of Earth Resources Satellites. Progress in Physical Geography 5(1), pp. 32-55.

TOWNSHEND, J.R.G. (1981b). Image Analysis and Interpretation for Land Resources Survey. In: Terrain Analysis and Remote Sensing, J.R.G. Townshend (editor), George Allen and Unwin, London, pp. 59-108.

TOWNSHEND, J.R.G. and JUSTICE, C.O. (1980). Unsupervised Classification of MSS Landsat Data for Mapping Spatially Complex Vegetation. International Journal of Remote Sensing 1(2), 105-120.

TOWNSHEND, J.R.G. and JUSTICE, C.O. (1981). Information Extraction from Remotely Sensed Data. International Journal of Remote Sensing 2(4), 313-329.

USGS (1979). Landsat Data User's Handbook, Revised Edition, United States Geological Survey, Arlington, Virginia.

WALKER, G.L. (1929). Surveying from the Air in Central Africa. Engineering and Mining Journal 127(2), 49-52.

WARD, J.M. (1969). The Significance of Changes in Infrared Reflectance in Sugar Maple (Acer saccharum Marsh), induced by soil conditions of drought and salinity. In: Proceedings of the 6th International Symposium on Remote Sensing of Environment, Ann Arbor, Michigan, Vol. 2, pp. 1205-1226.

WARREN, H.V. and DELAVAULT, R.E. (1949). Further Studies in Biogeochemistry. Bulletin of the Geological Society of America 60, 531-560.

WARREN, H.V., DELAVAULT, R.E. and FORTESCUE, J.A.C. (1955). Sampling in Biogeochemistry. Bulletin of the Geological Soceity of America 66, 229-238.

WIEGAND, C.L., GAUSMAN, W. and ALLEN, W.A. (1972). Physiological Factors and Optical Parameters as Bases of Vegetation Discrimination and Stress Analysis. In: Proceedings of the Seminar of Operational Remote Sensing, American Society of Photogrammetry, Falls Church, Virginia, pp. 82-102.

WILLIAMS, Jr., R.S. and CARTER, W.D. (1976) ERTS-1, A New Window on Our Planet. U.S. Geological Survey Professional Paper 929, 362 pp.

WOOLEY, J.T. (1971). Reflectance and Transmittance of Light by Leaves. Plant Physiology 47, 656-662.

YOST, E. and WENDEROTH, S. (1971). The Reflectance Spectra of Mineralized Trees. In: Proceedings of the 7th International Symposium on Remote Sensing of Environment, Ann Arbor, Michigan, Vol. 1, pp. 269-284.

YOST, E. (1975). Multispectral Color Photography for Mineral Exploration by Remote Sensing of Biogeochemical Anomalies. NASA-CR-144811, N77-10606, 147 pp.

YOUNES, H.A., ABDEL-AAL, R.M., KHODAIR, M.M. and ABDEL-SAMIE, A.G. (1974). Spectral Reflectance Studies on Mineral Deficiency in Corn Plants. In: Proceedings of the 9th International Symposium on Remote Sensing of Environment, Ann Arbor, Michigan, Vol. 2, pp. 1105-1125.